

Peaks within peaks and the possible two-peak structure of the $P_c(4457)$: The effective field theory perspective

Fang-Zheng Peng,¹ Jun-Xu Lu,¹ Mario Sánchez Sánchez,² Mao-Jun Yan,¹ and Manuel Pavon Valderrama^{1,3,*}

¹*School of Physics, Beihang University, Beijing 100191, China*

²*Centre d'Études Nucléaires, CNRS/IN2P3, Université de Bordeaux, 33175 Gradignan, France*

³*International Research Center for Nuclei and Particles in the Cosmos and Beijing Key Laboratory of Advanced Nuclear Materials and Physics, Beihang University, Beijing 100191, China*



(Received 10 August 2020; accepted 7 December 2020; published 21 January 2021)

The LHCb pentaquarks—the $P_c(4312)$, $P_c(4440)$, and $P_c(4457)$ —have been theorized to be $\Sigma_c \bar{D}$ and $\Sigma_c \bar{D}^*$ S-wave molecules. Here, we explore the possibility that two of these pentaquarks—the $P_c(4440)$ and $P_c(4457)$ —contain in addition a $\Lambda_c(2595)\bar{D}$ component in the P-wave. We will analyze the effects of this extra channel within two effective field theories: the first one will be a standard contact-range effective field theory, and the second one will include the nondiagonal pion dynamics connecting the $\Sigma_c \bar{D}^*$ and $\Lambda_c(2595)\bar{D}$ channels, which happens to be unusually long ranged. The impact of the coupled-channel dynamics between the $\Sigma_c \bar{D}^*$ and $\Lambda_c(2595)\bar{D}$ components is modest at best for the $P_c(4440)$ and $P_c(4457)$, which will remain predominantly $\Sigma_c \bar{D}^*$ molecules. However, if the quantum numbers of the $P_c(4457)$ are $J^P = \frac{1}{2}^-$, the coupled-channel dynamics is likely to induce the binding of a $\Lambda(2595)\bar{D}$ S-wave molecule (coupled to $\Sigma_c \bar{D}^*$ in the P-wave) with $J^P = \frac{1}{2}^+$ and a mass similar to the $P_c(4457)$. If this is the case, the $P_c(4457)$ could actually be a double peak containing two different pentaquark states.

DOI: [10.1103/PhysRevD.103.014023](https://doi.org/10.1103/PhysRevD.103.014023)

I. INTRODUCTION

The discovery of three pentaquark peaks—the $P_c(4312)$, $P_c(4440)$, and $P_c(4457)$ —by the LHCb Collaboration [1] raises the question of what is their nature. A commonly invoked explanation is that they are $\Sigma_c \bar{D}$ and $\Sigma_c \bar{D}^*$ bound states [2–9], which comes naturally from the closeness of the pentaquark peaks to the corresponding baryon-meson thresholds and also from the existence of theoretical predictions predating their observation [10–16]. Yet the evidence that they are molecular is mostly circumstantial at the moment, and other explanations might very well be possible [17–21].

In this paper, we will explore a modified molecular interpretation of the $P_c(4440)$ and $P_c(4457)$ pentaquarks and the consequences it entails. Of course, the fundamental idea will still be that these two pentaquarks are hadronic bound states, but besides the standard $\Sigma_c \bar{D}^*$ interpretation, we will also consider the existence of a $\Lambda_c(2595)\bar{D}$ ($\Lambda_{c1}\bar{D}$ from now on) component for the $P_c(4440)$ and $P_c(4457)$.

In the isospin-symmetric limit, the $\Sigma_c \bar{D}^*$ and $\Lambda_{c1}\bar{D}$ thresholds are located at 4462.2 and 4459.5 MeV, respectively, very close to the masses of the $P_c(4440)$ and $P_c(4457)$. Thus, it is natural to wonder whether the $\Lambda_{c1}\bar{D}$ channel plays a role in the description of the pentaquarks.

This idea was originally proposed by Burns [8], who conjectured that the $\Lambda_{c1}\bar{D}$ component might be important for the binding of molecular pentaquarks. Later, it was realized that the pion-exchange dynamics mediating the $\bar{D}^* \Sigma_c \rightarrow \bar{D} \Lambda_{c1}$ transition is unusually long ranged and in practice takes the form of a $1/r^2$ potential [22]. This is indeed a really interesting potential in the sense that it can display discrete scale invariance when attractive enough [23–25], which in turn opens the possibility of the existence of hadronic molecules for which there is a geometric spectrum reminiscent of the Efimov effect in the three-boson system [26]. For the hidden charm pentaquarks, the strength of the $1/r^2$ potential is probably not enough to trigger a geometric molecular spectrum [22], yet this might very well happen in other two-hadron molecular systems. Recently, Burns and Swanson have considered the $\bar{D}^* \Sigma_c \rightarrow \bar{D} \Lambda_{c1}$ pion-exchange dynamics beyond its long-distance behavior, leading to the conclusion that the $P_c(4457)$ might not be a $\frac{1}{2}^- \bar{D}^* \Sigma_c$ S-wave molecular state but a $\frac{1}{2}^+ \bar{D} \Lambda_{c1}$ one instead [8].

The present paper delves further into the consequences that a $\bar{D} \Lambda_{c1}$ component will have for the pentaquark

*mpavon@buaa.edu.cn

Published by the American Physical Society under the terms of the [Creative Commons Attribution 4.0 International license](https://creativecommons.org/licenses/by/4.0/). Further distribution of this work must maintain attribution to the author(s) and the published article's title, journal citation, and DOI. Funded by SCOAP³.

spectrum. For this, we formulate two effective field theories (EFTs): a pionless EFT and a *half-pionful* EFT. By *half-pionful*, we denote an EFT which includes the unusually long-ranged pion dynamics of the $\bar{D}^*\Sigma_c \rightarrow \bar{D}\Lambda_{c1}$ transition, for which the characteristic length scale is between 10 and 20 fm, but does not include the pion dynamics of the $\bar{D}^*\Sigma_c$ system, which has a range in between 1 and 2 fm. We find that the addition of the $\bar{D}\Lambda_{c1}$ channel is inconsequential if the quantum numbers of the $P_c(4440)$ and $P_c(4457)$ molecular pentaquarks are $\frac{1}{2}^-$ and $\frac{3}{2}^-$, respectively. However, if the quantum numbers of the $P_c(4457)$ pentaquark are $\frac{1}{2}^-$ instead, then the existence of a partner state with a similar mass and quantum numbers $\frac{1}{2}^+$ is very likely. That is, the $P_c(4457)$ might be a double peak, as happened with the original $P_c(4450)$ pentaquark discovered in 2015 [27].

The manuscript is structured as follows. In Sec. II, we explain how to describe the $\bar{D}\Sigma_c$, $\bar{D}\Sigma_c^*$, and $\bar{D}\Lambda_{c1}$ interactions within a pionless contact-range EFT. In Sec. III, we introduce the half-pionful theory, in which we include the pion exchange transition potential in the $\bar{D}\Sigma_c^*-\bar{D}\Lambda_{c1}$ channel. In Sec. IV, we revisit the description of the LHCb pentaquark trio within the previous two EFTs. Finally, in Sec. V, we present our conclusions.

II. PIONLESS THEORY

In this section, we will derive the lowest-order (LO) contact-range interaction for the $\bar{D}^*\Sigma_c-\bar{D}\Lambda_{c1}$ system. By *pionless theory*, we specifically refer to an EFT in which pions are subleading, instead of an EFT without pions; while the latter is the usual meaning of pionless in the nuclear sector (see, e.g., Refs. [28,29]), in the hadronic sector we are often constrained to LO calculations. Thus, it makes sense to use the word pionless to describe the LO EFT only, which is the part of the theory that we will be using. For formulating the LO contact-range Lagrangian, we will find it convenient to use the *light-quark notation* explained in detail in Ref. [30], which has been previously used in the literature, e.g., in Refs. [16,31]. In contrast with the standard superfield notation (see, for instance, Ref. [32] for a clear exposition) in which we combine heavy hadrons with the same light-quark spin into a unique superfield, in the light-quark notation, we simply write the interactions in terms of the light-quark spin degrees of freedom within the heavy hadrons. Of course, both notations are equivalent, but for nonrelativistic problems, the light-quark notation is easier to use.

A. $\bar{D}\Sigma_c$ and $\bar{D}^*\Sigma_c$ channels

The \bar{D} and \bar{D}^* charmed antimesons are $\bar{Q}q$ states where the light quark q and heavy antiquark \bar{Q} are in the S-wave. From heavy-quark spin symmetry, we expect the heavy-antiquark to effectively behave as a static color source, which in practical terms means that the wave function of the

light quark is independent of the total spin of the S-wave heavy meson. That is, the light-quark wave function (the “brown muck”) of the \bar{D} and \bar{D}^* charmed antimesons is the same [modulo corrections coming from the heavy-antiquark mass m_Q , which scale as Λ_{QCD}/m_Q , with $\Lambda_{\text{QCD}} \sim (200\text{--}300)$ MeV the QCD scale]. Two possible formalisms to express this symmetry are the standard heavy-superfield notation and the light-subfield notation. In the former, we combine the \bar{D} and \bar{D}^* field into a single superfield [32],

$$H_{\bar{Q}} = \frac{1}{\sqrt{2}} [\bar{D} + \vec{\sigma} \cdot \vec{D}^*], \quad (1)$$

where the superfield is well behaved with respect to heavy-antiquark rotations

$$H_{\bar{Q}} \rightarrow e^{i\vec{S}_H \cdot \vec{\theta}} H_{\bar{Q}}, \quad (2)$$

with \vec{S}_H representing the heavy-antiquark spin operator and $\vec{\theta}$ representing the rotation axis and angle. Thus, the combination of $H_{\bar{Q}}^\dagger$ and $H_{\bar{Q}}$ superfields in the Lagrangian effectively results in invariance with respect to heavy-antiquark rotations, i.e., to heavy-antiquark spin.

Conversely, in the light-subfield (or light-quark) notation, we prescind of writing down the heavy antiquark explicitly and instead express everything in terms of the effective light-quark degrees of freedom within the charmed antimeson and the light-quark spin operator,

$$\bar{D}, \bar{D}^* \rightarrow q_L, \vec{\sigma}_L, \quad (3)$$

where q_L represents an effective light-quark subfield, i.e., a field with the quantum numbers of the light quark within the charmed antimeson.¹ Then, we write down explicit rules for transforming the light-quark spin operator into charmed antimeson spin operators

$$\langle \bar{D} | \vec{\sigma}_L | \bar{D} \rangle = 0, \quad (4)$$

$$\langle \bar{D} | \vec{\sigma}_L | \bar{D}^* \rangle = \vec{e}_1, \quad (5)$$

$$\langle \bar{D}^* | \vec{\sigma}_L | \bar{D}^* \rangle = \vec{S}_1, \quad (6)$$

where \vec{e}_1 is the polarization vector of the \bar{D}^* meson and \vec{S}_1 is the spin-1 matrices.

Regarding the Σ_c and Σ_c^* charmed baryons, their quark content is Qqq where the qq diquark has light spin $S_L = 1$ and the system is in the S-wave. The structure of the

¹The q_L field does not represent an actual light-quark field q , but the effective field that results from ignoring the heavy-quark spin degree of freedoms within the charmed antimeson.

S-wave charmed baryons is independent of whether the baryon spin is $S = \frac{1}{2} (\Sigma_c)$ or $\frac{3}{2} (\Sigma_c^*)$. In the standard heavy-superfield notation, this is taken into account by defining the superfield [33]

$$\vec{S}_Q = \frac{1}{\sqrt{3}} \vec{\sigma} \Sigma_c + \vec{\Sigma}_c^*, \quad (7)$$

which has good heavy-quark rotation properties, while in the light-quark notation, we simply write everything in terms of the light-diquark subfield a_L (i.e., the qq pair) and its light-spin operator

$$\Sigma_c, \Sigma_c^* \rightarrow a_L, \vec{S}_L, \quad (8)$$

where a_L is the field representing the effective light-diquark degrees of freedom (with quantum numbers $J^P = 1^+$, i.e., an axial vector), with the translation rules

$$\langle \Sigma_c | \vec{S}_L | \Sigma_c \rangle = \frac{2}{3} \vec{\sigma}_2, \quad (9)$$

$$\langle \Sigma_c | \vec{S}_L | \Sigma_c^* \rangle = \frac{1}{\sqrt{3}} \vec{S}_2, \quad (10)$$

$$\langle \Sigma_c^* | \vec{S}_L | \Sigma_c^* \rangle = \frac{2}{3} \vec{\Sigma}_2, \quad (11)$$

where $\vec{\sigma}_2$ are the Pauli matrices as applied to the charmed baryon Σ_c , \vec{S} is a set of the matrices representing the spin- $\frac{1}{2}$ to spin- $\frac{3}{2}$ transition (which can be consulted in Ref. [34]), and $\vec{\Sigma}_2$ are the spin- $\frac{3}{2}$ matrices.

With these ingredients, the interaction between a \bar{D} charmed antimeson and a Σ_c charmed baryon can be easily written as

$$\mathcal{L}_1 = C_a (q_L^\dagger q_L) (a_L^\dagger a_L) + C_b (q_L^\dagger \vec{\sigma}_L q_L) \cdot (a_L^\dagger \vec{S}_L a_L), \quad (12)$$

which leads to the nonrelativistic contact-range potential

$$V_{C1} = C_a + C_b \vec{\sigma}_{L1} \cdot \vec{S}_{L2}. \quad (13)$$

This potential can be particularized for the two cases of interest for us in the present work, the $\bar{D}\Sigma_c$ and $\bar{D}^*\Sigma_c$ systems

$$V_{C1}(\bar{D}\Sigma_c) = C_a, \quad (14)$$

$$V_{C1}(\bar{D}^*\Sigma_c) = C_a + C_b \frac{2}{3} \vec{S}_1 \cdot \vec{\sigma}_2, \quad (15)$$

which we will use for the $P_c(4312)$ and the $\bar{D}^*\Sigma_c$ components of the $P_c(4440)$ and $P_c(4457)$, respectively.

B. $\bar{D}^*\Sigma_c - \bar{D}\Lambda_{c1}$ transition

Now, we will consider the $\bar{D}^{(*)}\Sigma_c^{(*)}$ to $\bar{D}^{(*)}\Lambda_{c1}^{(*)}$ transitions, which are necessary for the description of the $\bar{D}\Lambda_{c1}$ component in the $P_c(4440)$ and $P_c(4457)$ pentaquarks. First, we will consider the structure of the Λ_{c1} and Λ_{c1}^* P-wave charmed baryons (where Λ_{c1}^* refers to the $\Lambda_c(2625)$), which are Qqq states in which the spin of the light-quark pair is $S_L = 0$ and their orbital angular momentum is $L_L = 1$, yielding a total angular momentum of $J_L = 1$. In practice, this means that there is no substantial difference (except for parity) between the description of the Σ_c , Σ_c^* and Λ_{c1} , Λ_{c1}^* charmed baryons either in terms of heavy-superfield or light-subfield notations. In the superfield notation, we will write [35]

$$\vec{R}_Q = \frac{1}{\sqrt{3}} \vec{\sigma} \Lambda_{c1} + \vec{\Lambda}_{c1}^*, \quad (16)$$

while in the light-quark notation, we use

$$\Lambda_{c1}, \Lambda_{c1}^* \rightarrow v_L, \vec{L}_L, \quad (17)$$

with v_L representing the light-diquark pair (with quantum numbers $J^P = 1^-$, i.e., a vector field) and \vec{L}_L being the spin-1 matrices, where we use a different notation than in the S-wave charmed-baryon case to indicate that the angular momentum comes from the orbital angular momentum of the light-quark pair. This does not entail any operational difference, with the translation rules being

$$\langle \Lambda_{c1} | \vec{L}_L | \Lambda_{c1} \rangle = \frac{2}{3} \vec{\sigma}_2, \quad (18)$$

$$\langle \Lambda_{c1} | \vec{L}_L | \Lambda_{c1}^* \rangle = \frac{1}{\sqrt{3}} \vec{S}_2, \quad (19)$$

$$\langle \Lambda_{c1}^* | \vec{L}_L | \Lambda_{c1}^* \rangle = \frac{2}{3} \vec{\Sigma}_2, \quad (20)$$

which are analogous to these of the Σ_c , Σ_c^* baryons; see Eqs. (9)–(11).

With these ingredients, we are ready to write the $\bar{D}^{(*)}\Sigma_c^{(*)} \rightarrow \bar{D}^{(*)}\Lambda_{c1}^{(*)}$ transition Lagrangian. If for simplicity we limit ourselves to the subset of operators generating a $D \rightarrow D^*$ transition, we find that at lowest order there are two independent relevant operators, which for convenience we write as

$$\begin{aligned} \mathcal{L}_2 = & D_a (q_L^\dagger \vec{\sigma}_L q_L) \cdot (v_L^\dagger \overleftrightarrow{\nabla} a_L) \\ & + i D_b (q_L^\dagger \vec{\sigma}_L q_L) \cdot (v_L^\dagger \vec{J}_L \times \overleftrightarrow{\nabla} a_L) + C.C., \end{aligned} \quad (21)$$

with $\overleftrightarrow{\nabla} = (\overrightarrow{\nabla} - \overleftarrow{\nabla})$ and where \vec{J}_L refers to the spin-1 matrices as applied between the light-diquark axial and

vector fields within the S- and P-wave charmed baryons. The translation rules for the \vec{J}_L operator happen to be

$$\langle \Sigma_c | \vec{J}_L | \Lambda_c \rangle = \frac{2}{3} \vec{\sigma}_2, \quad (22)$$

$$\langle \Sigma_c | \vec{J}_L | \Lambda_c^* \rangle = \frac{1}{\sqrt{3}} \vec{S}_2, \quad (23)$$

$$\langle \Sigma_c^* | \vec{J}_L | \Lambda_c^* \rangle = \frac{2}{3} \vec{S}_2, \quad (24)$$

which are analogous to Eqs. (9)–(11) and (18)–(20), except that now the initial and final baryon states are different (either the S- to P-wave baryon transition or vice versa). Other operators choices are possible in the Lagrangian of Eq. (21), but the present one is particularly useful because the D_a term is pionlike, while the D_b term is ρ -like; they are similar to what we could get from the exchange of a pion and a ρ , respectively, as we explain in the Appendix. The potential we obtain is

$$V_{C2}(1 \rightarrow 2) = +D_a \vec{\sigma}_{L1} \cdot \vec{q} + iD_b \vec{q} \cdot (\vec{\sigma}_{L1} \times \vec{J}_{L2}), \quad (25)$$

while in the other direction, it is

$$V_{C2}(2 \rightarrow 1) = -D_a \vec{\sigma}_{L1} \cdot \vec{q} + iD_b \vec{q} \cdot (\vec{\sigma}_{L1} \times \vec{J}_{L2}), \quad (26)$$

where D_a and D_b are real in the convention we have used to write the potentials. It is important to notice that V_{C2} is a nondiagonal potential and can be redefined by a phase

$$V_{C2}(1 \rightarrow 2) \rightarrow e^{+i\phi} V_{C2}(1 \rightarrow 2), \quad (27)$$

$$V_{C2}(2 \rightarrow 1) \rightarrow e^{-i\phi} V_{C2}(2 \rightarrow 1), \quad (28)$$

in which case the potential is still self-adjoint. In the convention above, the p-space partial wave projection is purely real, while the r-space partial wave projection is purely imaginary. To avoid the inconveniences originating from this fact, when working in coordinate space, we will automatically add the phase $\phi = \pm\pi$ for the nondiagonal potential to be real.

Phenomenologically, we expect the D_a and D_b couplings to represent the exchange of a pseudoscalar and vector mesons, respectively. However, there is no short-range contribution directly attributable to a pseudoscalar meson; pion exchange is excessively long ranged as to be included in the contact-range potential. For taking this into account, we will devise a power counting in which the D_a coupling is a subleading-order contribution, while D_b remains leading. Thus, the effective potential we will use from now on will be

$$V_{C2} = iD_b \vec{q} \cdot (\vec{\sigma}_{L1} \times \vec{S}_{L2}). \quad (29)$$

C. $\bar{D}\Lambda_{c1}$ channel

Finally, we consider the $\bar{D}^{(*)}\Lambda_{c1}^{(*)}$ system, which enters the description of the $P_c(4440)$ and $P_c(4457)$ as an additional (P-wave) component of the wave function. Yet, this meson-baryon system is particularly relevant for a theoretical pentaquark with quantum numbers $J^P = \frac{1}{2}^+$, for which the most important meson-baryon component of the wave function will be $\bar{D}\Lambda_{c1}$ in the S-wave.

The lowest-order interaction in the $\bar{D}^*\Lambda_{c1}^*$ system happens to be formally identical to the one for the $\bar{D}^{(*)}\Sigma_c^{(*)}$ system, that is,

$$\mathcal{L}_3 = E_a(q_L^\dagger q_L)(v_L^\dagger v_L) + E_b(q_L^\dagger \vec{\sigma}_L q_L) \cdot (v_L^\dagger \vec{L}_L v_L), \quad (30)$$

which leads to the potential

$$V_{C3} = E_a + E_b \vec{\sigma}_{L1} \cdot \vec{L}_{L2}. \quad (31)$$

If we particularize to the $\bar{D}\Lambda_{c1}$ molecule, we will end up with

$$V_{C3}(\bar{D}\Lambda_{c1}) = E_a, \quad (32)$$

which is a really simple potential, where the coupling E_a is unknown.

D. Partial-wave projection

For the partial-wave projection of the contact-range potentials (and the one pion exchange (OPE) potential later on), we will use the spectroscopic notation $^{2S+1}L_J$ to denote a state with spin S , orbital angular momentum L , and total angular momentum J . For the pentaquarks states, we are considering— P_c , P_c' , and P_c^* —the relevant partial waves are

$$P_c \left(\frac{1^-}{2} \right) : ^2S_{1/2}(\bar{D}\Sigma_c), \quad (33)$$

$$P_c' \left(\frac{1^+}{2} \right) : ^2S_{1/2}(\bar{D}\Lambda_{c1}) - ^2P_{1/2}(\bar{D}^*\Sigma_c) - ^4P_{1/2}(\bar{D}^*\Sigma_c), \quad (34)$$

$$P_c^* \left(\frac{1^-}{2} \right) : ^2S_{1/2}(\bar{D}^*\Sigma_c) - ^2P_{1/2}(\bar{D}\Lambda_{c1}), \quad (35)$$

$$P_c^* \left(\frac{3^-}{2} \right) : ^4S_{3/2}(\bar{D}^*\Sigma_c) - ^2P_{3/2}(\bar{D}\Lambda_{c1}), \quad (36)$$

where we indicate the relevant meson-baryon channels within parentheses.

E. Momentum-space representation

For the momentum-space representation, we simply project the relevant contact-range potential into the partial waves of interest. For the P_c ($\bar{D}\Sigma_c$) pentaquark, we simply have

$$\langle p' | V(P_c) | p \rangle = C_a. \quad (37)$$

Next, for the two P_c^* configurations ($J = \frac{1}{2}, \frac{3}{2}$), we have

$$\langle p' | V\left(P_c^*, \frac{1}{2}\right) | p \rangle = \begin{pmatrix} C_a - \frac{4}{3}C_b & \frac{2}{\sqrt{3}}\frac{2D_b}{3}p \\ \frac{2}{\sqrt{3}}\frac{2D_b}{3}p' & 0 \end{pmatrix}, \quad (38)$$

$$\langle p' | V\left(P_c^*, \frac{3}{2}\right) | p \rangle = \begin{pmatrix} C_a + \frac{2}{3}C_b & -\frac{1}{\sqrt{3}}\frac{2D_b}{3}p \\ -\frac{1}{\sqrt{3}}\frac{2D_b}{3}p' & 0 \end{pmatrix}. \quad (39)$$

Finally, for the P_c' ($\bar{D}\Lambda_{c1}$) pentaquark, we have

$$\langle p' | V(P_c') | p \rangle = \begin{pmatrix} E_a & -\frac{2}{\sqrt{3}}\frac{2D_b}{3}p & -\sqrt{\frac{2}{3}}\frac{2D_b}{3}p \\ -\frac{2}{\sqrt{3}}\frac{2D_b}{3}p' & 0 & 0 \\ -\sqrt{\frac{2}{3}}\frac{2D_b}{3}p' & 0 & 0 \end{pmatrix}, \quad (40)$$

which can be simplified to a two-channel form if we take into account that the two P-wave $\bar{D}^*\Sigma_c$ components can adopt the configuration

$$\frac{2}{\sqrt{6}}|\bar{D}^*\Sigma_c(2P_{1/2})\rangle + \frac{1}{\sqrt{3}}|\bar{D}^*\Sigma_c(4P_{1/2})\rangle, \quad (41)$$

which maximizes the strength of the transition potential and we end up with

$$\langle p' | V(P_c') | p \rangle = \begin{pmatrix} E_a & -\sqrt{2}\frac{2D_b}{3}p \\ -\sqrt{2}\frac{2D_b}{3}p' & 0 \end{pmatrix}. \quad (42)$$

Notice that this simplification is only possible for the pionless theory at LO; if we include pion exchanges or other effects, we will have to revert to the original three-channel representation.

F. Coordinate-space representation

We obtain the r-space contact-range potential from Fourier-transforming the p-space one,

$$V(\vec{r}) = \int \frac{d^3\vec{q}}{(2\pi)^3} V(\vec{q}) e^{-i\vec{q}\cdot\vec{r}}, \quad (43)$$

which in the case of the V_{C1} and V_{C3} potentials leads to

$$V_{C1}(\vec{r}) = (C_a + C_b \vec{\sigma}_{L1} \cdot \vec{S}_{L2}) \delta^{(3)}(\vec{r}), \quad (44)$$

$$V_{C3}(\vec{r}) = (E_a + E_b \vec{\sigma}_{L1} \cdot \vec{L}_{L2}) \delta^{(3)}(\vec{r}). \quad (45)$$

For the V_{C2} potential, which contains one unit of orbital angular momentum, the transformation is a bit more involved, resulting in

$$V_{C2}(1 \rightarrow 2) = [+iD_a \vec{\sigma}_{L1} \cdot \vec{\nabla} - D_b \vec{\nabla} \cdot (\vec{\sigma}_{L1} \times \vec{J}_{L2})] \delta^{(3)}(\vec{r}), \quad (46)$$

which can be further simplified by rewriting

$$\vec{\nabla} \delta^{(3)}(\vec{r}) = \hat{r} \partial_r \delta^{(3)}(\vec{r}), \quad (47)$$

leading to

$$V_{C2}(1 \rightarrow 2) = [+iD_a \vec{\sigma}_{L1} \cdot \hat{r} - D_b \hat{r} \cdot (\vec{\sigma}_{L1} \times \vec{J}_{L2})] \partial_r \delta^{(3)}(\vec{r}). \quad (48)$$

This last expression is particularly useful because the partial wave projection of the $\vec{\sigma}_{L1} \cdot \hat{r}$ and $\hat{r} \cdot (\vec{\sigma}_{L1} \times \vec{J}_{L2})$ is identical to their p-space versions. Finally, we redefine $V_{C2}(1 \rightarrow 2)$ by a phase to end up with a purely real potential:

$$V_{C2}(1 \rightarrow 2) \rightarrow -iV_{C2}(1 \rightarrow 2). \quad (49)$$

With the previous conventions and the power counting, we use (for which D_a is a subleading-order effect), we end up with the r-space potentials

$$V(\vec{r}; P_c) = C_a \delta^{(3)}(\vec{r}), \quad (50)$$

$$V\left(\vec{r}; P_c^*, \frac{1}{2}\right) = \begin{pmatrix} C_a - \frac{4}{3}C_b & \frac{2}{\sqrt{3}}\frac{2D_b}{3}\partial_r \\ \frac{2}{\sqrt{3}}\frac{2D_b}{3}\partial_r & 0 \end{pmatrix} \delta^{(3)}(\vec{r}), \quad (51)$$

$$V\left(\vec{r}; P_c^*, \frac{3}{2}\right) = \begin{pmatrix} C_a + \frac{2}{3}C_b & -\frac{1}{\sqrt{3}}\frac{2D_b}{3}\partial_r \\ -\frac{1}{\sqrt{3}}\frac{2D_b}{3}\partial_r & 0 \end{pmatrix} \delta^{(3)}(\vec{r}), \quad (52)$$

$$V(\vec{r}; P_c') = \begin{pmatrix} E_a & -\sqrt{2}\frac{2D_b}{3}\partial_r \\ -\sqrt{2}\frac{2D_b}{3}\partial_r & 0 \end{pmatrix} \delta^{(3)}(\vec{r}), \quad (53)$$

where for the P_c' pentaquark we have written the simplified two-channel version of the potential.

G. Regularization and renormalization

The contact-range potentials we are using are not well defined unless we include a regulator to suppress the

unphysical high-momentum components of the potential. For the p-space version of the potential, this is done with the substitution

$$\langle p'|V_C|p\rangle \rightarrow \langle p'|V_{C,\Lambda}|p\rangle f\left(\frac{p'}{\Lambda}\right) f\left(\frac{p}{\Lambda}\right), \quad (54)$$

with $f(x)$ a regulator function, for which we will choose a Gaussian, $f(x) = e^{-x^2}$. For the r-space version of the potential, we will use a delta-shell regulator

$$\delta^{(3)}(\vec{r}) \rightarrow \frac{\delta(r - R_c)}{4\pi R_c^2}, \quad (55)$$

$$\partial_r \delta^{(3)}(\vec{r}) \rightarrow \frac{3}{R_c} \frac{\delta(r - R_c)}{4\pi R_c^2}, \quad (56)$$

with R_c the coordinate-space cutoff, where the $3/R_c$ factor in the derivative of the delta is chosen for its Fourier transform to be either p or p' in the $R_c \rightarrow 0$ limit after the partial wave projection.

H. Dynamical equation

For finding the location of the bound states, we have to iterate the r- or p-space potentials that we have obtained within a dynamical equation. For the r-space potential, we will solve the reduced Schrödinger equation

$$-u_a'' + \sum_b 2\mu_b V_{ab}(r) u_b(r) + \frac{L_a(L_a + 1)}{r^2} u_a(r) = -\gamma_a^2 u_a(r), \quad (57)$$

where a and b are indices we use to represent the different channels in the molecules we are considering as detailed in Eqs. (33)–(36), while V_{ab} is the potential between two channels, see Eqs. (50)–(53), which is regularized as in Eqs. (55) and (56). The reduced mass, angular momentum, and wave number of a given channel a are represented by μ_a , L_a , and γ_a . In turn, the wave number is given by $\gamma_a = \sqrt{2\mu_a(M_{th(a)} - M)}$, with $M_{th(a)}$ the mass of the two-hadron threshold for channel a and M the mass of the molecular pentaquark we are predicting.

For the p-space potential, we will solve the Lippmann-Schwinger equation as applied to the pole of the T-matrix, that is,

$$\phi_a(\vec{p}) = \sum_b \int \frac{d^3\vec{q}}{(2\pi)^3} \frac{\langle \vec{p}|V_{ab}|\vec{q}\rangle}{M_{th(b)} - M - \frac{q^2}{2\mu_b}} \phi_b(\vec{q}), \quad (58)$$

where a and b represent the channel; ϕ_a is the vertex function for channel a (where the vertex function is related to the residue of the T-matrix); V_{ab} is the potential between two channels, see Eqs. (37)–(40), which is regularized according to Eq. (54); and M is the mass of the molecular

pentaquark, while $M_{th(a)}$ and μ_a are the two-hadron threshold and the reduced mass for a given channel a .

III. HALF-PIONFUL THEORY

The exchange of one pion between the $\bar{D}^*\Sigma_c$ and $\bar{D}\Lambda_{c1}$ channels has the particularity that its range is extremely enhanced. The reason is that the pion in the $\Sigma_c\Lambda_{c1}\pi$ and $D^*D\pi$ vertices can be emitted or absorbed almost on the mass shell, resulting in an improved range. Besides, owing to the opposite parity of the Σ_c and Λ_{c1} baryons, the pion exchange in this vertex is in the S-wave. In combination with the standard P-wave pion in the vertex involving the charmed mesons, the outcome is that, instead of having a central and tensor forces with orbital angular momentum $L = 0$ and 2 , respectively, we end up with a vector force with $L = 1$. The long-range behavior of the vector force is $1/r^2$, i.e., an inverse square-law potential, which can trigger a series of interesting theoretical consequences when the strength of the potential is above a certain critical value [22]. Yet, as explained in Ref. [22], this is probably not the case for the LHCb pentaquarks as hadronic molecules.

Now, we begin by writing the pion-exchange Lagrangians for the Σ_c to Λ_{c1} transition in the heavy superfield notation:

$$\mathcal{L}_{HH\pi} = \frac{g_1}{\sqrt{2}f_\pi} \text{Tr}[H_Q^\dagger \tau_a \vec{\sigma} \cdot \vec{\nabla} \pi_a H_Q], \quad (59)$$

$$\mathcal{L}_{RS\pi} = \frac{h_2}{f_\pi} \vec{R}_Q^\dagger t_a \partial_0 \pi_a \cdot \vec{S}_Q + C.C., \quad (60)$$

which are obtained from the nonrelativistic limits of the Lagrangians of Refs. [32,35]. The light-quark notation version happens to be trivial,

$$\mathcal{L}_{q_L q_L \pi} = \frac{g_1}{\sqrt{2}f_\pi} q_L^\dagger \tau_a \vec{\sigma}_L \cdot \vec{\nabla} \pi_a q_L, \quad (61)$$

$$\mathcal{L}_{e_L d_L \pi} = \frac{h_2}{f_\pi} v_L^\dagger t_a \partial_0 \pi_a a_L + C.C. \quad (62)$$

From the previous Lagrangians, we can derive the OPE potential in momentum space, which reads as follows,

$$V_{\text{OPE}}(\vec{q}, 1 \rightarrow 2) = \frac{g_1 h_2}{\sqrt{2}f_\pi^2} \vec{\tau}_1 \cdot \vec{\tau}_2 \frac{\omega_\pi \vec{\sigma}_{L1} \cdot \vec{q}}{\vec{q}^2 + \mu_\pi^2}, \quad (63)$$

where we are indicating that this is the transition potential in the $\bar{D}^{(*)}\Sigma_c^{(*)} \rightarrow \bar{D}^{(*)}\Lambda_{c1}^{(*)}$ direction. The operator $\vec{\tau}_1 \cdot \vec{\tau}_2 = \sqrt{3}$ for total isospin $I = \frac{1}{2}$ and 0 otherwise. The equivalent expression in coordinate space can be obtained by Fourier transforming the previous expression, where in addition we include a phase to follow the convention of having a purely real transition potential,

$$V_{\text{OPE}}(\vec{r}, 1 \rightarrow 2) = \vec{\tau}_1 \cdot \vec{t}_2 \vec{\sigma}_{L1} \cdot \hat{r} W_E(r), \quad (64)$$

with W_E defined as

$$W_E(r) = \frac{g_1 h_2 \omega_\pi \mu_\pi^2 e^{-\mu_\pi r}}{4\pi \sqrt{2} f_\pi^2 \mu_\pi r} \left(1 + \frac{1}{\mu_\pi r} \right). \quad (65)$$

For the couplings, we have taken $g_1 = 0.59$ (as deduced from the $D^* \rightarrow D\pi$ and $D^* \rightarrow D\gamma$ decays [36,37]), $h_2 = 0.63$ (from the analysis of Ref. [38], where h_2 is extracted from $\Gamma(\Lambda_{c1} \rightarrow \Sigma_c \pi)$ as measured by CDF [39]), $f_\pi = 130$ MeV, and $\omega_\pi \simeq (m(\Lambda_{c1}) - m(\Sigma_1)) \simeq (m(D^*) - m(D)) \simeq m_\pi$, with $m_\pi = 138$ MeV. Finally, $\mu_\pi = \sqrt{m_\pi^2 - \omega_\pi^2} \simeq 0$, a value we will further discuss in the following lines.

A. Infrared regularization

In the $\mu_\pi \rightarrow 0$ limit, which is close to the physical situation we are dealing with and will probably represent a good approximation of it, the previous OPE potential becomes a $1/r^2$ infinite-range potential. In particular, the p-space potential reads

$$V_{\text{OPE}}(\vec{q}, 1 \rightarrow 2) \rightarrow \frac{g_1 h_2}{\sqrt{2} f_\pi^2} \vec{\tau}_1 \cdot \vec{t}_2 \frac{\omega_\pi \vec{\sigma}_{L1} \cdot \vec{q}}{q^2}, \quad (66)$$

while for the r-space potential, we can take this approximation into account within the function W_E ,

$$W_E(r) \rightarrow \frac{g_1 h_2 \omega_\pi}{4\pi \sqrt{2} f_\pi^2} \frac{1}{r^2}. \quad (67)$$

Of course, this is merely an approximation. What is actually happening is that the modulus of the effective pion mass $|\mu_\pi|$ will be in general considerably smaller than the pion mass m_π (or any other hadronic scale for that matter). We have $|\mu_\pi| \sim (10\text{--}20)$ MeV, its concrete value depending on the specific particle channel under consideration. In a few particle channels, μ_π is purely imaginary, indicating the possibility of decay into the $\bar{D}\Sigma_c \pi$ channel, and in others, it

is real. A detailed treatment of these difference is, however, outside the scope of the present manuscript.

Here, we will opt for the much easier treatment we were describing above, that is, to assume that $\mu_\pi = 0$. For taking into account that the range of the OPE potential is actually not infinite, we will include an infrared cutoff. For the partial-wave projection of OPE in momentum space, we will introduce an infrared cutoff Λ_{IR} in the following way,

$$\langle p' | V_{\text{OPE}} | p \rangle \rightarrow \langle p' | V_{\text{OPE}} | p \rangle \theta(|q_-| - \Lambda_{\text{IR}}) \theta(|q_+| - \Lambda_{\text{IR}}), \quad (68)$$

with $q_- = p - p'$ and $q_+ = p + p'$, with the infrared cutoff chosen within the cutoff window $\Lambda_{\text{IR}} = (10\text{--}20)$ MeV, which corresponds with the size of the modulus of the effective pion mass. In coordinate space, the inclusion of the infrared cutoff R_{IR} will be considerably simpler

$$V_{\text{OPE}}(\vec{r}) \rightarrow V_{\text{OPE}}(\vec{r}) \theta(R_{\text{IR}} - r), \quad (69)$$

where we will take $R_{\text{IR}} = (10\text{--}20)$ fm.

Actually, the effect of this infrared cutoff is only important if the strength of the $1/r^2$ potential is equal to or larger than the critical value triggering a geometric spectrum. This does not happen for any of the pentaquarks we are considering, at least with the currently known values of the couplings g_1 and h_2 . However, in the P'_c pentaquark, the strength is not far away from that critical value [22], indicating that in this case the results will have a larger dependence on the infrared cutoff.

B. Partial-wave projection

The partial-wave projection of the OPE potential is trivial for its coordinate-space representation; owing to its clear separation into a radial and angular piece—Eq. (64)—it merely requires considering the partial wave projection of the vector operator $\vec{\sigma}_{L1} \cdot \vec{r}$, which we already showed in Table I.

For the momentum-space representation of the potential, the partial-wave projection is a bit more complex, yet it can be written as

TABLE I. Matrix elements of the vector operators for the partial waves we are considering in this work.

Molecule	Partial waves	J^P	$\vec{\sigma}_{L1} \cdot \hat{r}$	$\hat{r} \cdot (\vec{\sigma}_{L1} \times \vec{S}_{L2})$
$\bar{D}\Lambda_{c1} - \bar{D}^* \Sigma_c$	${}^2S_{1/2} - {}^2P_{1/2} - {}^4P_{1/2}$	$\frac{1}{2}^+$	$\begin{pmatrix} 0 & +\frac{1}{\sqrt{3}} & -\sqrt{\frac{2}{3}} \\ +\frac{1}{\sqrt{3}} & 0 & 0 \\ -\sqrt{\frac{2}{3}} & 0 & 0 \end{pmatrix}$	$\begin{pmatrix} 0 & \frac{2i}{\sqrt{3}} & i\sqrt{\frac{2}{3}} \\ -\frac{2i}{\sqrt{3}} & 0 & 0 \\ -i\sqrt{\frac{2}{3}} & 0 & 0 \end{pmatrix}$
$\bar{D}^* \Sigma_c - \bar{D}\Lambda_{c1}$	${}^2S_{1/2} - {}^2P_{1/2}$	$\frac{1}{2}^-$	$\begin{pmatrix} 0 & \frac{1}{\sqrt{3}} \\ \frac{1}{\sqrt{3}} & 0 \end{pmatrix}$	$\begin{pmatrix} 0 & -\frac{2i}{\sqrt{3}} \\ +\frac{2i}{\sqrt{3}} & 0 \end{pmatrix}$
$\bar{D}^* \Sigma_c - \bar{D}\Lambda_{c1}$	${}^4S_{3/2} - {}^2P_{3/2}$	$\frac{3}{2}^-$	$\begin{pmatrix} 0 & \frac{1}{\sqrt{3}} \\ \frac{1}{\sqrt{3}} & 0 \end{pmatrix}$	$\begin{pmatrix} 0 & +\frac{i}{\sqrt{3}} \\ -\frac{i}{\sqrt{3}} & 0 \end{pmatrix}$

$$\begin{aligned} \langle p'(^S L'_J) | V | p(^S L_J) \rangle &= \frac{g_1 h_2}{\sqrt{2} f_\pi^2} \vec{\tau}_1 \cdot \vec{\tau}_2 \omega_\pi \langle ^S L'_J | \vec{\sigma}_{L1} \cdot \hat{q} | ^S L_J \rangle \\ &\times \langle p'(L') | \frac{1}{|\vec{q}|} | p(L) \rangle, \end{aligned} \quad (70)$$

where the matrix elements of the vector operator are again to be found in Table I, to which we have to add the partial wave projection of the $1/|\vec{q}|$ potential:

$$\begin{aligned} \langle p'(1) | \frac{1}{|\vec{q}|} | p(0) \rangle &= \frac{2\pi}{p'} \left[1 + \frac{p'^2 - p^2}{2pp'} \log \left| \frac{p + p'}{p - p'} \right| \right], \\ \langle p'(0) | \frac{1}{|\vec{q}|} | p(1) \rangle &= \frac{2\pi}{p} \left[1 + \frac{p^2 - p'^2}{2pp'} \log \left| \frac{p + p'}{p - p'} \right| \right]. \end{aligned} \quad (71)$$

Of course, we still supplement the previous expressions with the infrared cutoff of Eq. (68).

IV. PENTAQUARK TRIO REVISITED

In this section, we consider the description of the $P_c(4312)$, $P_c(4440)$, and $P_c(4457)$ pentaquarks within the EFTs proposed in this work. We will begin by reviewing their standard molecular interpretations as $\bar{D}\Sigma_c$ and $\bar{D}^*\Sigma_c$ bound states, and then we will move to the novel molecular interpretation in which the $\bar{D}\Lambda_{c1}$ channel is included as an explicit degree of freedom for the $P_c(4440)$ and $P_c(4457)$ pentaquarks. The prediction of a $\bar{D}\Lambda_{c1}$ bound state is contingent on an unknown coupling constant, E_a . For dealing with this issue, we will consider two different estimations of the value of this coupling and the predictions they will entail.

A. Standard molecular interpretation

We begin by reviewing the standard molecular interpretation of Ref. [5], in which the pentaquarks were considered to be $\bar{D}\Sigma_c$ and $\bar{D}^*\Sigma_c$ molecules (without any $\bar{D}\Lambda_{c1}$ component) described by a pionless EFT. This pionless EFT is equivalent to using the V_{C1} contact-range potential of Eq. (13), which contains two independent couplings C_a and C_b . The original procedure [5] for determining these two couplings was as follows:

- (i) Use the $P_c(4440)$ and $P_c(4457)$ as $\bar{D}^*\Sigma_c$ molecules to determine the C_a and C_b couplings.
- (ii) Postdict the $P_c(4312)$ as a $\bar{D}\Sigma_c$ molecule, and compare with its experimental location.

For convenience, we will modify the previous procedure in this manuscript:

- (i) Use the $P_c(4312)$ and $P_c(4457)$ as $\bar{D}\Sigma_c$ and $\bar{D}^*\Sigma_c$ molecules to determine the C_a and C_b couplings.
- (ii) Postdict the $P_c(4440)$ as a $\bar{D}^*\Sigma_c$ molecule, and compare with its experimental location.

This choice guarantees that the prediction of the pentaquark trio remain all below their respective meson-baryon thresholds; the later inclusion of the $\bar{D}\Lambda_{c1}$ channel can in a few

instances move the $P_c(4457)$ a bit above the threshold for hard cutoffs if we fit the couplings as in Ref. [5].

Now, for the $\bar{D}^*\Sigma_c$ molecules, there are two spin configurations, $J = \frac{1}{2}$ and $\frac{3}{2}$, but we do not know which one corresponds to each of the pentaquarks. As a consequence, we consider two scenarios, A_0 and B_0 :

- (a) in scenario A_0 , the $P_c(4440)$ has $J = \frac{1}{2}$, while the spin of the $P_c(4457)$ is $J = \frac{3}{2}$,
- (b) in scenario B_0 , the $P_c(4440)$ has $J = \frac{3}{2}$, while the spin of the $P_c(4457)$ is $J = \frac{1}{2}$,

where we use the subscript ‘‘zero’’ to indicate that this is the base case in which the $\bar{D}\Lambda_{c1}$ channel is not included. Then, we postdict the location of the $P_c(4440)$ in each scenario, resulting in

$$M_{A_0} = 4440.1(4434.5) \text{ MeV}, \quad (72)$$

$$M_{B_0} = 4449.6(4447.6) \text{ MeV} \quad (73)$$

for the p-space Gaussian regulator with $\Lambda = 0.5(1.0)$ GeV and

$$M_{A_0} = 4438.9(4433.8) \text{ MeV}, \quad (74)$$

$$M_{B_0} = 4449.3(4447.5) \text{ MeV} \quad (75)$$

for the r-space delta-shell regulator with $R = 1.0(0.5)$ fm. These numbers are to be compared with the experimental value $M = (4440.3 \pm 1.3_{-4.6}^{+4.1})$ MeV, which indicates that scenario A_0 is preferred over scenario B_0 (particularly for softer cutoffs). This coincides with the conclusions of the previous pionless EFT of Ref. [5]. Yet, it should be noted that this is a LO calculation, and hence we should expect a sizable truncation error, which can be estimated by comparing the predictions at different cutoffs, for instance. The cutoff variation indicates a $\Delta M = 2.0\text{--}5.6$ MeV uncertainty for the masses of the pentaquarks; see Eqs. (72)–(75). Once we consider this uncertainty, both scenarios A and B happen to be compatible with the experimental location of the pentaquarks. For comparison purposes, we notice that EFT calculations including the $\bar{D}^*\Sigma_c$ pion dynamics [7,9], which we have considered here to be a subleading-order effect and thus part of ΔM , tend to prefer scenario B .

B. Novel molecular interpretation

Now, we explore the novel molecular interpretation we propose, in which the $P_c(4312)$ is a $\bar{D}\Sigma_c$ molecule while the $P_c(4440)$ and $P_c(4457)$ are $\bar{D}^*\Sigma_c\text{--}\bar{D}\Lambda_{c1}$ molecules. The contact-range piece of the potential for the pionless and half-pionful EFTs is given by Eqs. (37)–(39), which contain three independent coupling constants (C_a , C_b , and D_b). Finally, we conjecture the existence of a $\bar{D}\Lambda_{c1}$ S-wave molecule, which we call the P'_c and for which the

contact-range piece of the potential is given by Eq. (40), which includes a new coupling (E_a).

Of these four couplings, we can determine three of them— C_a , C_b , and D_b —from the masses of the three pentaquarks. The procedure we will follow is:

- (i) Use the $P_c(4312)$ as a $\bar{D}\Sigma_c$ molecule to determine the C_a coupling.
- (ii) Use the $P_c(4440)$ and $P_c(4457)$ as $\bar{D}^*\Sigma_c\bar{D}\Lambda_{c1}$ molecules to determine the C_b and D_b couplings.
- (iii) If there is no solution for the previous procedure, we will set $D_b = 0$, and, as in the uncoupled-channel case, we will determine C_b from the condition of reproducing the $P_c(4457)$ pole.
- (iv) Finally, we determine for which values of E_a the P'_c (the conjectured S-wave $\bar{D}\Lambda_{c1}$ molecule) binds and compare these values with expectations from naive dimensional analysis (NDA).

As in the standard molecular interpretation, we have two possible scenarios which we now call A_1 and B_1 , where A_1 (B_1) corresponds to the $P_c(4457)$ being a $J = \frac{3}{2}$ ($\frac{1}{2}$) molecule. We will further subdivide the scenario A_1 (B_1) into a pionless and a half-pionful version, which we will denote A_1^π (B_1^π) and A_1^π (B_1^π), respectively. It happens that the couplings can be compared with NDA, in particular D_b and E_a ; the D_b comparison can provide an indirect estimation of the likelihood of scenarios A_1 and B_1 , while E_a will provide the binding likelihood of the P'_c pentaquark.

To illustrate this idea, we can consider the pionless p-space calculation, which for $\Lambda = 0.5$ GeV in scenario A_1^π and B_1^π gives

$$C_a = -2.17 \text{ fm}^2, \quad (76)$$

$$C_b = +0.55 \text{ fm}^2 (A_1^\pi), \quad (77)$$

$$D_b = +0.00 \text{ fm}^2 (A_1^\pi), \quad (78)$$

$$C_b = -0.85 \text{ fm}^2 (B_1^\pi), \quad (79)$$

$$D_b = +0.99 \text{ fm}^2 (B_1^\pi). \quad (80)$$

This translates into the following condition for the P'_c to bind

$$E_a \leq -1.13 \text{ fm}^2 (A_1^\pi), \quad (81)$$

$$E_a \leq +0.04 \text{ fm}^2 (B_1^\pi), \quad (82)$$

which in scenario A_1^π requires the coupling E_a to be attractive, while scenario B_1^π will lead to binding even for a slightly repulsive coupling. For the calculation, we have used the following values for the masses of the hadrons involved, $m(D) = 1867.22$ MeV, $m(D^*) = 2008.61$ MeV,

$m(\Sigma_c) = 2453.54$ MeV, $m(\Lambda_{c1}) = 2592.25$ MeV, which are the isospin averages of the PDG values [40].

A complete list of the couplings can be consulted in Table III for the different EFTs and regulators considered in this work. Independently of the choice of regulator and cutoff, the binding of the P'_c pentaquark is much more probable in scenario B_1 (pionless or half-pionful). In scenario A_1 , there is no pair of values for the C_b and D_b couplings that simultaneously reproduces the $P_c(4440)$ and $P_c(4457)$ pentaquarks, and thus we have set $D_b = 0$ and followed the same procedure as in scenario A_0 to determine C_b . We will further comment on why this happens later on in this section.

Now, we can compare the previous numbers with the NDA estimation of the expected size of a contact-range coupling,

$$|C_{l,l'}| \sim |c_{l,l'}| \frac{4\pi}{M^{l+l'+2}}, \quad (83)$$

where l, l' are the angular momenta of the initial and final states that the contact-range potential couples, M is the hard scale of the theory, and $c_{l,l'} \sim \mathcal{O}(1)$ is a numerical factor of order 1 related to the partial wave projection. The origin of this estimation deserves further discussion. On the one hand, we have the $1/M^{l+l'+2}$ scaling, which comes from the canonical dimension of the contact-range coupling, i.e., $[C_{l,l'}] = [\text{mass}]^{-l-l'-2}$. On the other hand, the numerical factors can be deduced from different heuristical arguments. Here, we will consider a simple argument based on matching the $C_{l,l'}$ coupling with the Fourier transform of an unknown, generic short-range potential characterized by the hard-range scale M , i.e.,

$$V_S(r) = Mg(Mr)e^{-Mr}, \quad (84)$$

where we are ignoring further dependence on the angular momentum for simplicity. The exponential decay indicates that this potential is generated by the exchange of a meson of mass M at short distances, while $g(x)$ is a function that depends on the details of the interaction with that meson. We expect $C_{l,l'}$ to be proportional to the Fourier transform of V_S at low energies, i.e.,

$$C_{l,l'} p^l p'^{l'} \propto \lim_{p,p' \rightarrow 0} \langle p'(l') | V_S | p(l) \rangle, \quad (85)$$

with the partial wave projection of the Fourier transform given by

$$\langle p'(l') | V_S | p(l) \rangle = 4\pi i^{l-l'} \int dr r^2 j_l(pr) V_S(r) j_{l'}(p'r), \quad (86)$$

with $j_l(x)$ the spherical Bessel function and V_S the short-range potential. From these two formulas, we can easily

trace back the 4π and $c_{l,l'}$ factors in Eq. (83); the 4π is simply a trivial consequence of writing the Fourier transform in the partial wave basis, while the $c_{l,l'}$ factor comes from the interplay between the low-momentum behavior of the spherical Bessel functions and the exponential decay of the short-range potential. For instance, if we consider the short-range S-wave and S-to-P-wave potentials generated by the exchange of a meson, the general form of the short-range potential V_S will probably be a Yukawa for the S-wave case and a derivative of a Yukawa for the S-to-P-wave transition [in the line of Eq. (65)]. If this is the case, the g functions in Eq. (84) will take the form

$$g_S(x) \propto \frac{1}{x} \quad \text{and} \quad g_{SP}(x) \propto \frac{1}{x} \left(1 + \frac{1}{x}\right), \quad (87)$$

which leads to the numerical factors $c_S \propto 1$ and $c_{SP} \propto 1$. Other arguments might lead to different estimations of the $c_{l,l'}$ factors, but we will expect most of them to converge toward $c_{l,l'} = \mathcal{O}(1)$. For a recent review about NDA in EFTs, we recommend Ref. [41], which further points out to $c_{l,l'} = \mathcal{O}(1)$. But we observe that most arguments are devoted to S-wave contact-range couplings, with comparatively less effort invested in the naturalness of the $l, l' \neq 0$ cases. The exception is Halo EFT [42], which is, however, focused on the more interesting non-natural cases. The bottom line is that the NDA estimates for C_S are more well established than for C_{SP} and thus conclusions based on the naturalness of C_{SP} are less robust than the ones based on C_S .

Here, we will choose $c_{l,l'} = 1$ for simplicity. For hadrons, we expect $M \sim 1$ GeV, which gives us the following estimations for an S-wave and S-to-P wave counterterms:

$$|C_S^{\text{NDA}}| \sim 0.49 \text{ fm}^2 \quad \text{and} \quad |C_{SP}^{\text{NDA}}| \sim 0.10 \text{ fm}^3. \quad (88)$$

From this, we see that C_a is unnatural (see Table II), which is to be expected for the coupling of a two-body system that binds [28,43], while C_b and D_b are closer to natural, though this depends on the cutoff. This is particularly true for D_b , see Table III, which is close to its NDA estimate for $\Lambda = 1.0$ GeV but not so for $\Lambda = 0.5$ GeV. This might be very well related to our choice of $M \sim 1$ GeV for the hard scale, though; had we chosen a smaller M , we would have ended up with a stronger case for the naturalness of D_b (particularly because of the $1/M^3$ scaling). Besides this, we can appreciate that in scenario A_1 the binding of the P'_c pentaquark is possible but not particularly probable, as the size of the coupling E_a that is required to bind is larger than the NDA expectation. In contrast, in scenario B_1 , the coupling E_a required to bind falls well within what is expected from NDA. Thus, in this second case, binding seems to be much more likely.

TABLE II. The contact-range couplings C_a , C_b , and E_a when the $\bar{D}^*\Sigma_c$ and $\bar{D}\Lambda_{c1}$ channels do not couple. C_a and C_b are obtained from the condition of reproducing the mass of the $P_c(4312)$ and $P_c(4457)$ as molecular pentaquarks in p and r space (as indicated by type of cutoff: Λ and R_c). Scenario A (and its variants) corresponds to considering that the spin parities of the $P_c(4440)$ and $P_c(4457)$ are $J^P = \frac{1}{2}^-$ and $\frac{3}{2}^-$, respectively, while scenario B corresponds to the opposite identification. E_a^{crit} is the critical value of the E_a coupling required for the uncoupled $\bar{D}\Lambda_{c1}$ system to bind.

Scenario	Λ (GeV)	C_a (fm ²)	C_b (fm ²)	E_a^{crit} (fm ²)
A_0	0.5	-2.17	+0.55	-1.13
A_0	1.0	-0.80	+0.13	-0.57
B_0	0.5	-2.17	-0.27	-1.13
B_0	1.0	-0.80	-0.07	-0.57

Scenario	R_c (fm)	C_a (fm ²)	C_b (fm ²)	E_a^{crit} (fm ²)
A_0	0.5	-0.81	+0.14	-0.58
A_0	1.0	-2.16	+0.53	-1.18
B_0	0.5	-0.81	-0.07	-0.58
B_0	1.0	-2.16	-0.26	-1.18

Regarding the P'_c pentaquark, we can deduce its probable mass from the NDA estimation of the E_a coupling, provided this coupling is attractive:

$$E_a^{\text{NDA}} \simeq -\frac{4\pi}{M^2}. \quad (89)$$

Within scenario B_1 , this estimation of the coupling consistently generates a shallow P'_c close to the $\bar{D}\Lambda_{c1}$ threshold, where the concrete predictions can be consulted in Table IV. Of course, the question is whether it is sensible to assume that the E_a coupling is attractive. We will examine the validity of this assumption in the next few lines.

C. Can we further pinpoint the location of the P'_c pentaquark?

Regarding E_a , it will be useful not only to determine its sign but also its size beyond the NDA estimation we have already used to argue the existence of the P'_c pentaquark. From arguments regarding the saturation of contact-range couplings by light mesons [34,44], the light-meson contributions to E_a can be divided into two components,

$$E_a = E_a^S + E_a^V, \quad (90)$$

which correspond to the scalar (σ) and vector (ω) meson contributions. The scalar and vector contributions are attractive and repulsive ($E_a^S < 0$ and $E_a^V > 0$), respectively. At first sight, this ambiguous result seems to indicate that we cannot determine the sign of E_a , yet this would be

TABLE III. The contact-range couplings C_a , C_b and D_b from the condition of reproducing the mass of the $P_c(4312)$ and $P_c(4457)$ as molecular pentaquarks in p and r space (as indicated by type of cutoff: Λ and R_c). Scenario A (and its variants) corresponds to considering that the spin-parities of the $P_c(4440)$ and $P_c(4457)$ are $J^P = \frac{1}{2}^-$ and $\frac{3}{2}^-$, respectively, while scenario B corresponds to the opposite identification. For the half-pionful EFT, i.e., scenarios A_1^π and B_1^π , the number displayed corresponds to the softer infrared cutoff, i.e., $\Lambda_{\text{IR}} = 10$ MeV and $R_{\text{IR}} = 20$ fm, while the number in parenthesis represents the difference with $\Lambda_{\text{IR}} = 20$ MeV and $R_{\text{IR}} = 10$ fm in the last significant digit (if any). E_a^{crit} is the critical value of the E_a coupling required for the coupled $\bar{D}\Lambda_{c1}$ system to bind.

Scenario	Λ (GeV)	C_a (fm ²)	C_b (fm ²)	D_b (fm ³)	E_a^{crit} (fm ²)
A_1^π	0.5	-2.17	+0.55	0	-1.13
A_1^π	1.0	-0.80	+0.12	0	-0.57
B_1^π	0.5	-2.17	-0.85	0.99	+0.04
B_1^π	1.0	-0.80	-0.15	0.13	-0.40
A_1^π	0.5	-2.17	+0.57	0	-1.04(2)
A_1^π	1.0	-0.80	+0.15	0	-0.50(1)
B_1^π	0.5	-2.17	-0.76	1.01	+0.18(1)
B_1^π	1.0	-0.80	-0.11	0.12	-0.35

Scenario	R_c (fm)	C_a (fm ²)	C_b (fm ²)	D_b (fm ³)	E_a^{crit} (fm ²)
A_1^π	0.5	-0.81	+0.12	0	-0.51
A_1^π	1.0	-2.16	+0.51	0	-1.06
B_1^π	0.5	-0.81	-0.14	0.09	-0.42
B_1^π	1.0	-2.16	-0.75	0.66	-0.15
A_1^π	0.5	-0.81	0.15	0	-0.52(2)
A_1^π	1.0	-2.16	0.55	0	-1.10(8)
B_1^π	0.5	-0.81	-0.17	0.09	-0.38(2)
B_1^π	1.0	-2.16	-0.68	0.67	-0.09(8)

premature. As a matter of fact, the same situation would have arisen had we applied this argument to the two-nucleon system, but it happens that the deuteron binds. The reason is that the scalar meson contributions have a longer range than the vector meson ones, leading to net attraction.

This seems to be the case not only in the two-nucleon system but also in the $\bar{D}\Lambda_c$ case; according to a recent calculation in the one-boson-exchange model [45], the $\bar{D}\Lambda_c$ system is not far away from binding. In fact, had we adapted the recent one-boson exchange model of Ref. [46] (originally intended for the $\bar{D}^{(*)}\Sigma_c^{(*)}$ molecules) to the $\bar{D}\Lambda_{c1}$ system, the system would not have bound, yet its two-body scattering length a_2 would have probably been unnaturally large

$$a_2^{\text{OBE}}(\bar{D}\Lambda_{c1}) = -24.1_{-\infty(+9.5)}^{+20.7} \text{ fm}, \quad (91)$$

TABLE IV. The mass of the P'_c pentaquark as deduced from the NDA estimate of the E_a coupling (assuming it is attractive) in scenarios A_1 and B_1 , both in the pionless and half-pionful theories. For reference, the $\bar{D}\Lambda_{c1}$ threshold is located at 4459.5 MeV in the isospin-symmetric limit. E_a^{crit} has the same meaning as in Table III.

Scenario	Λ (MeV)	E_a^{crit} (fm ²)	E_a^{NDA} (fm ²)	$M^{\text{NDA}}(P'_c)$
A_1^π	0.5	-1.13	-0.49	...
A_1^π	1.0	-0.57	-0.49	...
B_1^π	0.5	+0.04	-0.49	4457.0
B_1^π	1.0	-0.40	-0.49	4457.9
A_1^π	0.5	-1.04(2)	-0.49	...
A_1^π	1.0	-0.50(1)	-0.49	...
B_1^π	0.5	+0.18(1)	-0.49	4456.3
B_1^π	1.0	-0.35	-0.49	4457.0

Scenario	R_c (fm)	E_a^{crit} (fm ²)	E_a^{NDA} (fm ²)	$M^{\text{NDA}}(P'_c)$
A_1^π	0.5	-0.58	-0.49	...
A_1^π	1.0	-1.18	-0.49	...
B_1^π	0.5	-0.42	-0.49	4458.1
B_1^π	1.0	-0.15	-0.49	4458.2
A_1^π	0.5	-0.52(2)	-0.49	...
A_1^π	1.0	-1.10(8)	-0.49	...
B_1^π	0.5	-0.38(2)	-0.49	4457.3
B_1^π	1.0	-0.09(8)	-0.49	4457.7

where the errors are computed as in Ref. [46] and are compatible with binding² (the lower error indicates that the scattering length changes sign, hence the $-\infty$, and that in that case its value would be +9.5 fm). This reinforces the conclusions derived from Ref. [45] for the $\bar{D}\Lambda_c$ case. That is, we expect $E_a < 0$ and close to the value required to have a shallow bound state in the absence of coupling with the $\bar{D}^*\Sigma_c$ channel. All this makes the P'_c pentaquark very likely in scenario B_1 , as we will now show with explicit calculations.

If we now describe the $\bar{D}\Lambda_{c1}$ two-body system in a pionless EFT, the coupling E_a can be determined from the value of the scattering length that we have already computed within the OBE model, leading to

$$E_a = -1.09_{-0.18}^{+0.21}(-0.55_{-0.04}^{+0.06}) \text{ fm}^2, \quad (92)$$

²The calculation assumes that the \bar{D} and Λ_{c1} hadrons are stable, which is not the case for the latter, but neither is this detail important as we take the scattering length as a proxy for determining the amount of attraction in the two-body system. The cutoff is taken as in Ref. [46], i.e., $\Lambda = 1.119_{-0.094}^{+0.190}$ GeV, while the couplings of the Λ_{c1} and Σ_c baryons to the σ and ω happen to be identical. Finally, Λ_{c1} does not couple to the ρ , owing to isospin.

for $\Lambda = 0.5(1.0)$ GeV if we do the calculations in p space, or alternatively

$$E_a = -1.10_{-0.19}^{+0.21}(-0.56_{-0.05}^{+0.06}) \text{ fm}^2, \quad (93)$$

for $R_c = 1.0(0.5)$ fm in r space. As already explained, this extracted value of the coupling is enough to guarantee a binding in scenario B_1 , both in the pionless and pionful versions. This would lead to a P'_c that is bound by (4–9) MeV depending on the case. The predicted locations can be found in Table V, where we have not only considered scenario B_1 (for which binding is more probable) but also scenario A_1 (for which binding can still happen in the half-pionful case). We can appreciate that in scenario B_1 the predictions are very similar, independently of the cutoff or whether the calculation has been done in r or p space. For a more graphical comparison, we have included Fig. 1, which shows the dependence of the binding energy on the coupling E_a for the half-pionful theory in momentum space for scenarios A_1 and B_1 . We have chosen this particular calculation as the representative case, as the

TABLE V. The mass of the P'_c pentaquark as deduced from the E_a coupling extracted from the OBE model in scenarios A_1 and B_1 , both in the pionless and half-pionful theory. For comparison, we remind the reader that the location of the $\bar{D}\Lambda_{c1}$ threshold in the isospin symmetric limit is 4459.5 MeV. E_a^{crit} has the same meaning as in Table III.

Scenario	Λ (GeV)	E_a^{crit} (fm ²)	E_a^{OBE} (fm ²)	$M^{\text{OBE}}(P'_c)$
A_1^π	0.5	-1.13	$-1.09_{-0.19}^{+0.21}$...
A_1^π	1.0	-0.57	$-0.55_{-0.04}^{+0.06}$...
B_1^π	0.5	+0.04	$-1.09_{-0.19}^{+0.21}$	$4451.2_{-2.2}^{+2.3}$
B_1^π	1.0	-0.40	$-0.55_{-0.04}^{+0.06}$	$4455.2_{-2.2}^{+2.7}$
A_1^π	0.5	-1.04(2)	$-1.09_{-0.19}^{+0.21}$	$4459.5_{-0.6}^\dagger$
A_1^π	1.0	-0.50(1)	$-0.55_{-0.04}^{+0.06}$	$4459.2_{-0.6}^\dagger$
B_1^π	0.5	+0.18	$-1.09_{-0.18}^{+0.21}$	$4450.3_{-2.1}^{+2.4}$
B_1^π	1.0	-0.35	$-0.55_{-0.04}^{+0.06}$	$4454.2_{-2.3}^{+2.7}$

Scenario	R_c (fm)	E_a^{crit} (fm ²)	E_a^{OBE} (fm ²)	$M^{\text{OBE}}(P'_c)$
A_1^π	0.5	-0.58	$-0.56_{-0.05}^{+0.06}$...
A_1^π	1.0	-1.18	$-1.10_{-0.19}^{+0.21}$...
B_1^π	0.5	-0.42	$-0.56_{-0.05}^{+0.06}$	$4455.2_{-2.6}^{+2.7}$
B_1^π	1.0	-0.15	$-1.10_{-0.19}^{+0.21}$	$4452.1_{-2.6}^{+2.5}$
A_1^π	0.5	-0.52(2)	$-0.56_{-0.05}^{+0.06}$	$4459.2(2)_{-1.0}^\dagger$
A_1^π	1.0	-1.10(8)	$-1.10_{-0.19}^{+0.21}$	$4459.5_{-0.6}^\dagger$
B_1^π	0.5	-0.38(2)	$-0.56_{-0.05}^{+0.06}$	$4454.3_{-2.4}^{+2.7}$
B_1^π	1.0	-0.09(8)	$-1.10_{-0.19}^{+0.21}$	$4451.5_{-2.5}^{+2.6}$

other three possible calculations in scenarios A_1 and B_1 would yield similar results (except that in the pionless theory scenario A_1 requires a larger $|E_a^{\text{crit}}|$ to bind). In Fig. 1, we also indicate the most probable values of E_a and the binding energy of the P'_c within a square.

At this point, it is important to notice that the estimations of the E_a coupling discussed here are not only close to binding for the $\bar{D}\Lambda_{c1}$ system but are also compatible with it once we take into account the theoretical uncertainties. This is not only true for the E_a coupling derived from the OBE model. For $\Lambda = 1.0$ GeV, the NDA estimation of E_a is not far away from the critical value required for binding, i.e., $|E_a^{\text{NDA}}| = 0.49 \text{ fm}^2$ to be compared with $E_a^{\text{crit}} = -0.57 \text{ fm}^2$. The bottom line is that, though the previous discussions have focused on scenario B , for which binding is more probable, the P'_c pentaquark could also exist in scenario A . That is, the difference between scenarios A and B regarding a possible $\bar{D}\Lambda_{c1}$ bound state is merely one of likelihood.

D. Can scenario A be discarded?

A preliminary examination of the different determinations of the couplings presented in Table III reveals that $D_b = 0$ in scenario A . The reason for this is that in general it is not possible to *exactly* reproduce the masses of the two $\bar{D}^*\Sigma_c$ pentaquarks in this scenario. This seems counterintuitive at first, but actually there are good reasons for this to be the case, which have to do with coupled-channel dynamics and which we will explain below. Of course, we stress here that we are referring to the exact matching of the three known pentaquark masses with the three parameters of the present EFT; provided D_b is smaller than its NDA estimate, the pentaquark trio is still well reproduced (particularly if we consider the experimental errors in the masses).

First, we will consider a molecular pentaquark P_Q in the heavy-quark limit, in which the masses of the charmed hadrons diverge and we can ignore the kinetic energy of the hadrons. In this limit, the binding energy of a molecular pentaquark is given by

$$B_{P_Q} = -\langle V^S \rangle, \quad (94)$$

where $\langle V^S \rangle$ is the expected value of the S-wave potential and where we have taken the convention that the binding energy B_{P_Q} is a positive number, thus the minus sign in front of $\langle V^S \rangle$. Now, we consider the case where the molecular pentaquark contains an additional P-wave component, for which the coupled-channel potential reads

$$V_{P_Q} = \begin{pmatrix} V^S & \lambda V^{SP} \\ \lambda V^{SP} & 0 \end{pmatrix}, \quad (95)$$

with V^{SP} the S-to-P-wave transition potential and λ a number describing the strength of the transition potential.

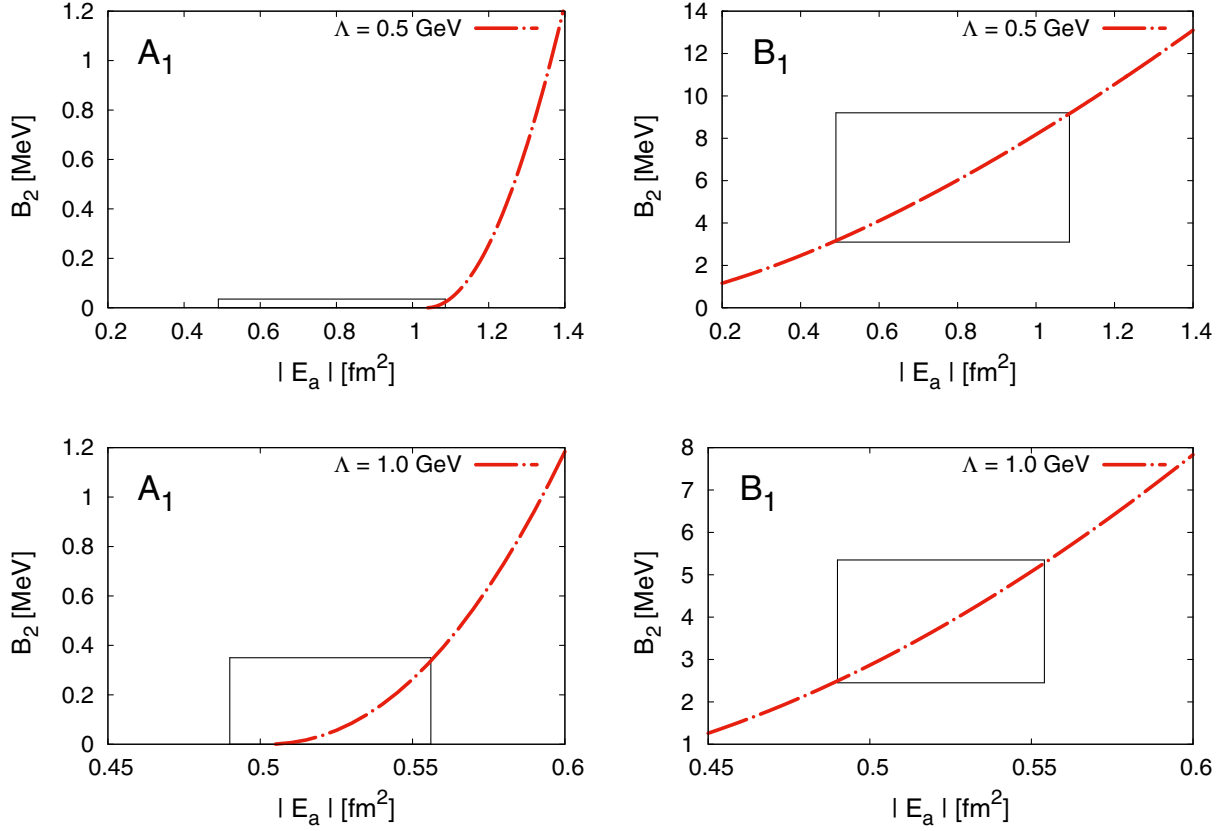


FIG. 1. Binding energy in scenarios A_1 and B_1 (p space) of the prospective P'_c pentaquark depending on the size of the coupling E_a . The square indicates what we consider to be the most probable values of the coupling E_a and the binding energy of the P'_c pentaquark; it comprises the values of E_a from the NDA to the OBE estimations, i.e., Eqs. (89) and (92). For scenario A_1 , the binding window is rather limited, 0–0.03 (0–0.3) MeV for $\Lambda = 0.5(1.0)$ GeV, where binding does not happen unless $|E_a|$ is above the critical values listed in Table V. For scenario B_1 , the most probable binding window is about 3.2–9.2 (2.5–5.3) MeV for $\Lambda = 0.5(1.0)$ GeV. For simplicity, we have only shown the half-pionful theory in momentum space (A_1^π and B_1^π), as the other cases considered in this work yield similar results (with the curves moving a bit toward the right in the pionless case).

If λ is small, the effect of the coupled-channel dynamics on the binding of the pentaquarks can be estimated in perturbation theory, leading to

$$B_{P_Q} = -\langle V^S \rangle - \lambda^2 \langle V^{SP} G_0 V^{SP} \rangle + \mathcal{O}(\lambda^3), \quad (96)$$

where G_0 is the two-hadron propagator, which in the static limit (infinitely heavy hadrons) reduces to

$$G_0 = \frac{1}{M_{P_Q} - M_{\text{th}}^P} = \frac{1}{\Delta^P}, \quad (97)$$

with M_{P_Q} the mass of the heavy pentaquark, M_{th}^P the location of the P-wave threshold, and Δ^P the energy gap. This simplifies the S-to-P-wave contribution to

$$B_{P_Q} = -\langle V^S \rangle - \lambda^2 \frac{\langle (V^{SP})^2 \rangle}{\Delta^P} + \mathcal{O}(\lambda^3), \quad (98)$$

which will increase the binding energy provided that $\Delta^P < 0$, which happens to be the case.³

The parameter λ is useful because it is proportional to the nondiagonal elements of the potentials in Eqs. (38)–(40). Thus, we have

$$\lambda^2 \propto \{6, 4, 1\}, \quad (99)$$

for the P'_c , $P_c^*(1/2)$, and $P_c^*(3/2)$ pentaquarks, respectively. The actual effect of the P-wave channel also depends on the inverse of the mass gap, i.e.,

$$\Delta B_{P_Q} \propto -\frac{\lambda^2}{\Delta^P}, \quad (100)$$

which implies that the impact of the $\bar{D}\Lambda_{c1}$ channel will be larger in the $P_c(4457)$ pentaquark than in the $P_c(4440)$ one

³Notice that we are assuming an attractive S-wave potential— $\langle V^S \rangle < 0$ —and that we always have $\langle (V^{SP})^2 \rangle \geq 0$.

($\Delta_p = -2.2$ and -19.2 MeV, respectively). However, once we take into account the finite mass of the hadrons, the effect of the mass gap on the $P_c(4457)$ will diminish in relative terms as it will be softened owing to the kinetic energy contributions.

In scenario *A*, the $P_c(4440)$ and $P_c(4457)$ are already well reproduced before including the $\bar{D}\Lambda_{c1}$ channel; i.e., the choice $D_b = 0$ is compatible with the experimental location of the pentaquarks without further modifications. Thus, it comes as no surprise that scenarios A_0 and A_1 are indistinguishable from the point of view of the couplings. Another factor to consider is the hyperfine splitting between the $P_c^*(1/2)$ and $P_c^*(3/2)$ pentaquarks, which in scenario A_0 is

$$M_{A_0}\left(\frac{3}{2}\right) - M_{A_0}\left(\frac{1}{2}\right) = 17.2(22.8) \text{ MeV}, \quad (101)$$

for the p-space Gaussian regulator with $\Lambda = 0.5(1.0)$ MeV, or

$$M_{A_0}\left(\frac{3}{2}\right) - M_{A_0}\left(\frac{1}{2}\right) = 18.5(24.0) \text{ MeV} \quad (102)$$

for the r-space delta-shell regulator with $R_c = 1.0(0.5)$ fm. This is to be compared with the experimental splitting $|\Delta| = 17.0^{+6.4}_{-4.7}$ MeV, where we have combined the errors of the pentaquark masses in quadrature. Now, it happens that the inclusion of the $\bar{D}\Lambda_{c1}$ channel widens the hyperfine splitting, as can be checked with the following calculation:

- (i) determine the C_a coupling from the location of the $P_c(4312)$ as a $\bar{D}\Sigma_c$ bound state (as usual),
- (ii) fix the coupling D_b to a predetermined value,
- (iii) determine C_b from the location $P_c(4457)$ as a $\bar{D}^*\Sigma_c - \bar{D}\Lambda_{c1}$ bound state,
- (iv) calculate the location of the $P_c(4440)$,

which is very similar to the procedures we have been following for scenarios A_0 and B_0 . The splitting we obtain for scenario *A* can be consulted in Fig. 2, where for simplicity we have only shown the pionless calculation in p space (the other calculations being qualitatively equivalent to this one). As can be appreciated in Fig. 2, the magnitude of the splitting grows with D_b , which in turn explains why it was not possible to find a solution in scenario A_1 . However, once we consider the errors in the pentaquark masses, scenario *A* is still compatible with the experimental location of the pentaquarks for small values of the coupling D_b . For the case of $\Lambda = 0.5(1.0)$ GeV, scenario *A* is compatible with experiment provided $|D_b| < 0.58(0.02) \text{ fm}^3$, which is to be compared with the NDA estimate $|D_b^{\text{NDA}}| = 0.10 \text{ fm}^3$. This indicates that NDA and scenario *A* are compatible for $\Lambda = 0.5$ GeV, but not for $\Lambda = 1.0$ GeV.

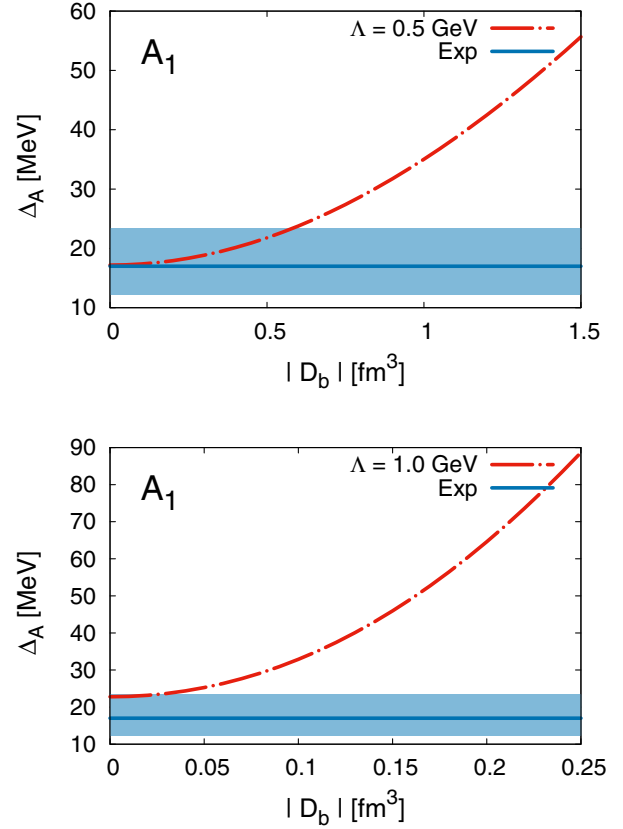


FIG. 2. Hyperfine splitting of the $P_c(4440)$ and $P_c(4457)$ pentaquarks in scenario *A* as a function of D_b . We define the mass splitting as $\Delta = M(P_c^*(\frac{3}{2})) - M(P_c^*(\frac{1}{2}))$, the sign of which is positive (negative) in scenario *A* (*B*). The blue band and blue line represent the experimental hyperfine splitting $|\Delta| = 17.0^{+6.4}_{-4.7}$. For simplicity, we have done the calculation in the pionless EFT for $\Lambda = 0.5$ and 1 GeV, with the other EFT variations yielding similar results.

For scenario *B*, the hyperfine splitting is

$$M_{B_0}\left(\frac{3}{2}\right) - M_{B_0}\left(\frac{1}{2}\right) = -7.7(-9.7) \text{ MeV}, \quad (103)$$

for the p-space Gaussian regulator with $\Lambda = 0.5(1.0)$ MeV, or

$$M_{B_0}\left(\frac{3}{2}\right) - M_{B_0}\left(\frac{1}{2}\right) = -8.1(-10.4) \text{ MeV}, \quad (104)$$

for the r-space delta-shell regulator with $R_c = 1.0(0.5)$ fm, to be compared with the -17.0 MeV figure which we obtain from the experimental masses. The inclusion of the $\bar{D}\Lambda_{c1}$ channel actually increases the absolute magnitude of the mass splitting, thus improving the agreement between theory and experiment. This can be seen in Fig. 3, where we show the hyperfine splitting as a function of the coupling D_b for scenario *B*. The details of the calculation are analogous to the ones we followed for Fig. 2.

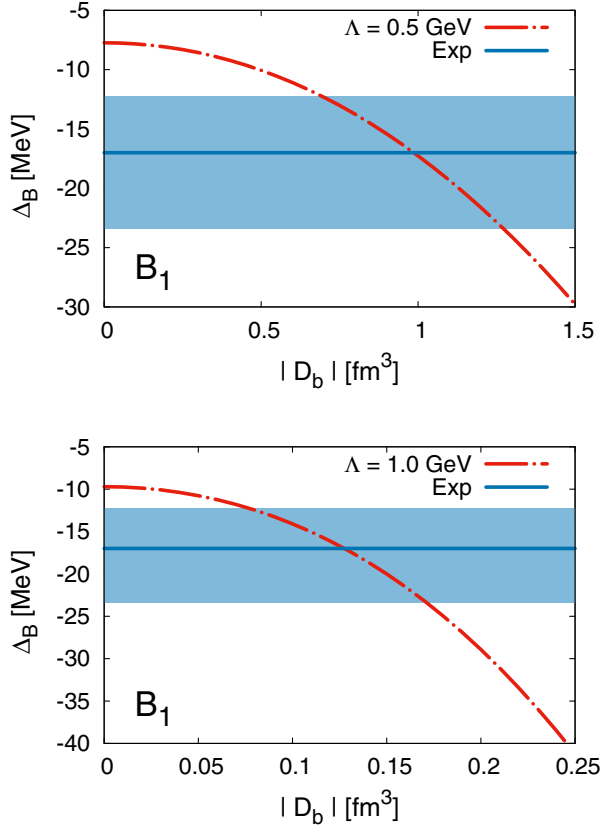


FIG. 3. Hyperfine splitting of the $P_c(4440)$ and $P_c(4457)$ pentaquarks in scenario B as a function of D_b . The conventions are identical as in Fig. 2, to which we refer for further details.

Compatibility with the size of the experimental splitting is possible for $0.70 \text{ fm}^3 < |D_b| < 1.26 \text{ fm}^3$ ($0.08 \text{ fm}^3 < |D_b| < 0.17 \text{ fm}^3$) for $\Lambda = 0.5(1.0) \text{ GeV}$. This indicates that scenario B agrees with the NDA estimates of D_b for $\Lambda = 1.0 \text{ GeV}$, while for $\Lambda = 0.5 \text{ GeV}$, it requires a D_b seven times the NDA estimate.

At this point, we observe that the NDA estimates for D_b seem to be better respected for $\Lambda = 1.0 \text{ GeV}$ than for $\Lambda = 0.5 \text{ GeV}$. We are not only referring to Figs. 2 and 3 but also to the couplings in Table III. Actually, this might be related to a series of factors, the most important one probably being that naturalness of contact-range interactions beyond S-waves has been rarely dealt with in the literature, except in Halo EFT [42] as previously noted. However, there are at least two reasons to revise the NDA estimates for D_b upward. The first one has to do with the numerical factors in front of D_b . The NDA estimate for $C_{l,l'}$ implicitly assumes a contact-range potential normalized as

$$\langle p'(l') | V_C | p(l) \rangle = C_{l,l'} p^{l'} p^l. \quad (105)$$

In contrast, the $\bar{D}^* \Sigma_c \rightarrow \bar{D} \Sigma_c$ transition potentials contain a factor in front of the coupling

$$\langle p'(0) | V_C | p(1) \rangle = \lambda \frac{2}{3\sqrt{3}} D_b p, \quad (106)$$

with λ a numerical factor that can be deduced from Eq. (99). Combining all the factors, this indicates that the NDA value of D_b should be 1.1–2.6 times the value of $C_{\text{SP}}^{\text{NDA}} = 0.10 \text{ fm}^3$, depending on which pentaquark we use as a reference. The second reason has to do with the choice of a hard scale M , for which we previously took the 1 GeV figure. Had we taken $M = m_\rho$ with $m_\rho = 770 \text{ MeV}$ the rho meson mass, we would have arrived at $C_{\text{SP}}^{\text{NDA}} = 0.21 \text{ fm}^3$, i.e., twice the estimation for $M = 1 \text{ GeV}$. Putting all these pieces together would suggest $D_b^{\text{NDA}} = (0.10\text{--}0.55) \text{ fm}^3$. But there could also be unaccounted for reasons for D_b to be smaller. The bottom line is that we still require external input to decide which scenario is more probable, be it phenomenological studies or further experiments.

Here, it is important to mention that the two theoretical scenarios we have presented (A and B) are but a subset of all the possible scenarios. We have three molecular explanations [$P_c^*(1/2)$, $P_c^*(3/2)$, and P_c'] for two pentaquarks, which gives a total of six possible scenarios instead of the two we are considering. But with the exception of scenarios A and B , it is not possible to determine the value of the couplings in other cases. For instance, had we assumed that the $P_c(4440)$ is the $J = \frac{3}{2} \bar{D}^* \Sigma_c$ molecule and $P_c(4457)$ is the $J = \frac{1}{2} \bar{D} \Lambda_{c1}$ one, i.e., the scenario originally proposed in Ref. [8], we would have ended with three unknown couplings (C_b , D_b , and E_a) for two pentaquarks. Though this limitation might indeed be overcome by invoking NDA, the resulting analysis is considerably more involved than in scenarios A and B , and thus we have decided not to consider them in this work.

Another factor that we have not taken into account in the present analysis is the effect of the $\bar{D} \Lambda_{c1}^*$ channel, which lies about 20 MeV above the $\bar{D} \Lambda_{c1}$ threshold. The $\bar{D} \Lambda_{c1}^*$ channel can mix with the $J = \frac{3}{2} \bar{D}^* \Sigma_c$ one, inducing a bit of extra attraction in this later case. However, from Eq. (100) and the larger mass gap for the $\bar{D} \Lambda_{c1}^*$ channel ($\Delta_p = -55.0 \text{ MeV}$ versus -19.2 MeV for the $\bar{D} \Lambda_{c1}$ one for scenario B), we expect this effect to be fairly modest.

V. CONCLUSIONS

In this paper, we have considered the impact of the $\bar{D} \Lambda_{c1}$ channel for the description of the $P_c(4440)$ and $P_c(4457)$ pentaquarks. Within the molecular picture, the standard interpretation of the $P_c(4440)$ and $P_c(4457)$ states is that they are $\bar{D}^* \Sigma_c$ bound states. This is motivated by the closeness of the $\bar{D}^* \Sigma_c$ threshold to the location of the two pentaquark states. But the same is true for the $\bar{D} \Lambda_{c1}$ threshold, which naturally prompts the question of what is the contribution of this channel to the description of the pentaquarks [8,22,47].

For answering this question, we have analyzed the inclusion of $\bar{D}\Lambda_{c1}$ channel from the EFT perspective. We find that the importance of the $\bar{D}\Lambda_{c1}$ channel depends on which are the quantum numbers of the $P_c(4440)$ and $P_c(4457)$ pentaquarks; in the standard molecular interpretation ($\bar{D}^*\Sigma_c$), their quantum numbers can be either $J^P = \frac{1}{2}^-$ or $\frac{3}{2}^-$, but we do not know which quantum numbers correspond to which pentaquark. There are two possibilities: that the $P_c(4440)$ and $P_c(4457)$ are, respectively, the $J^P = \frac{1}{2}^-$ and $\frac{3}{2}^-$ $\bar{D}^*\Sigma_c$ molecules, or vice versa. The first possibility, which we call scenario A, corresponds to the standard expectation that hadron masses increase with spin. The second possibility, scenario B, represents the opposite pattern, which has recently been conjectured to be a property of hadronic molecules [44].

In scenario A, the inclusion of the $\bar{D}\Lambda_{c1}$ channel is inconsequential for the description of the molecular pentaquarks; the $\bar{D}\Lambda_{c1}$ can effectively be ignored, as the transition potential between the $\bar{D}\Lambda_{c1} \rightarrow \bar{D}^*\Sigma_c$ channels is required to be weak if we want to reproduce the three known pentaquarks. However, this is not the case in scenario B, where the inclusion of the $\bar{D}\Lambda_{c1}$ channel can potentially have important consequences on the pentaquark spectrum. In this case, the coupling between the $\bar{D}\Lambda_{c1}$ and $\bar{D}^*\Sigma_c$ channels might very well be strong enough to facilitate the binding of the $\bar{D}\Lambda_{c1}$ system in the S-wave, as happened in Ref. [8]. Right now, there is no experimental determination of the quantum numbers of the pentaquarks, with different theoretical explorations favoring different scenarios. We see a preference toward A in Refs. [5,6] and toward B in Refs. [7,9,48,49], though other scenarios are possible; for instance, in Ref. [8], the $\frac{1}{2}^-$ $\bar{D}^*\Sigma_c$ pentaquark does not bind. Within the molecular picture, there seems to be a tendency for pionless theories to favor A, while theories that include pion exchange effects tend to fall into scenario B.

If scenario B happens to be the one preferred by nature, the prospects for the $J^P = \frac{1}{2}^+$ $\bar{D}\Lambda_{c1}$ molecule to bind are good; though the fate of this bound state is ultimately contingent on the unknown short-distance details of the interaction, phenomenological arguments indicate a moderate attraction between the \bar{D} meson and Λ_{c1} baryon at short distances. If this is the case and this molecule binds, it might very well be that the $P_c(4457)$ is a double peak, containing both a $\bar{D}^*\Sigma_c$ and a $\bar{D}\Lambda_{c1}$ molecule with opposite parities. If scenario A is the one that actually describes the pentaquarks, the $J^P = \frac{1}{2}^+$ pentaquark cannot be discarded either—there is the possibility that it binds even without coupling to the $\bar{D}^*\Sigma_c$ channel—but is less likely to exist, nonetheless.

Yet, we stress the exploratory nature of the present manuscript: the EFT framework requires experimental input

and a series of assumptions for it to be able to generate predictions. Indeed, there could be three pentaquarks independently of the quantum numbers of the experimentally observed ones, with scenario B merely being the case for which this possibility is more probable. In this regard, it would be very welcome to have phenomenological explorations of the $\bar{D}\Lambda_{c1}$ interaction and the $\bar{D}\Lambda_{c1} \rightarrow \bar{D}^*\Sigma_c$ transition.

ACKNOWLEDGMENTS

This work is partly supported by the National Natural Science Foundation of China under Grants No. 11735003 and No. 11975041, the Fundamental Research Funds for the Central Universities, and the Thousand Talent Plan for Young Professionals.

APPENDIX: PION- AND RHO-LIKE COUPLINGS

In this Appendix, we discuss the possible sources of saturation of the D_a and D_b contact-range couplings that mediate the $\bar{D}^*\Sigma_c \rightarrow \bar{D}\Lambda_{c1}$ transition.

Regarding the coupling D_a , its similarity with the exchange of a pseudoscalar is evident from a direct comparison to the contact-range potential of Eq. (25) for $D_b = 0$, that is,

$$V_{C2(a)}(1 \rightarrow 2) = +D_a \vec{\sigma}_{L1} \cdot \vec{q}, \quad (\text{A1})$$

and the OPE potential of Eq. (63). Saturation of the D_a coupling from a derivative pseudoscalar meson such as the pion will lead to the approximation [34,44]

$$D_a^{(\pi)} \propto \frac{g_1 h_2}{\sqrt{2} f_\pi^2} \vec{\tau}_1 \cdot \vec{\tau}_2 \frac{\omega_\pi}{\mu_\pi^2}. \quad (\text{A2})$$

However, saturation is only known to work if the regularization scale is close to the mass of the exchanged meson [50]. Taking into account that the pion is the lightest meson and that the cutoff range we are using is $\Lambda = (0.5-1.0)$ GeV, we do not expect the D_a coupling to receive contributions coming from pion exchange. If we consider the exchange of heavier mesons, there is no clear candidate for the exchange of a pseudoscalar meson in the mass range comprised by our choice of a cutoff, hence the decision to consider that $D_a = 0$ at lowest order.

For the D_b coupling, the situation is different because the $\bar{D}^*\Sigma_c \rightarrow \bar{D}\Lambda_{c1}$ transition can happen via rho-exchange. The relevant Lagrangians read

$$\mathcal{L}_{\rho 1} = g_{\rho 1} q_L^\dagger \tau_a \rho_{a0} q_L - \frac{f_{\rho 1}}{4M} \epsilon_{ijk} q_L^\dagger \sigma_{L,k} \tau_a \cdot (\partial_i \rho_{aj} - \partial_j \rho_{ai}) q_L, \quad (\text{A3})$$

$$\mathcal{L}_{\rho 2} = \frac{f_{\rho 2}}{2M} v_L^\dagger t_a (J_{Li} \partial_i \rho_a^0 - \partial_0 \rho_{ai}) a_L + C.C. \quad (\text{A4})$$

where q_L , a_L , and v_L are the light subfields of the $D^{(*)}$, $\Sigma_c^{(*)}$, and $\Lambda_{c1}^{(*)}$ charmed hadrons; $\rho_{a\mu}$ is the rho meson field, with μ a Lorentz index (i is used to indicate $\mu = 1, 2, 3$) and a and isospin index; t_a and τ_a are isospin matrices; $g_{\rho 1}$, $f_{\rho 1}$, and $f_{\rho 2}$ are coupling constants; and M is a mass scale for the magnetic and electric dipole terms (i.e., the piece proportional to $f_{\rho 1}$ and $f_{\rho 2}$, respectively). The chargelike term (i.e., the one proportional to $g_{\rho 1}$) can contribute to $\bar{D}\Sigma_c \rightarrow \bar{D}\Lambda_{c1}$ and $\bar{D}^*\Sigma_c \rightarrow \bar{D}^*\Lambda_{c1}$ transitions but not to the $\bar{D}^*\Sigma_c \rightarrow \bar{D}\Lambda_{c1}$ one, which is of interest for this work. The magnetic and electric and dipole terms of these Lagrangian lead to the potential

$$V_\rho(\vec{q}, 1 \rightarrow 2) = \frac{f_{\rho 1} f_{\rho 2}}{2M 2M} \vec{\tau}_1 \cdot \vec{\tau}_2 \frac{\omega_\rho}{\vec{q}^2 + \mu_\rho^2} \vec{q} \cdot (\vec{\sigma}_{L1} \times \vec{J}_{L2}), \quad (\text{A5})$$

where $\omega_\rho \simeq (m(\Lambda_{c1}) - m(\Sigma_c)) \simeq (m(D^*) - m(D))$, $\mu_\rho^2 = m_\rho^2 - \omega_\rho^2$ and the rest of the terms have the same meaning as in Eqs. (25) and (63). Finally, the saturation of the D_b coupling by the rho will lead to a value proportional to

$$D_b^{(\rho)} \propto \frac{f_{\rho 1} f_{\rho 2}}{2M 2M} \vec{\tau}_1 \cdot \vec{\tau}_2 \frac{\omega_\rho}{\mu_\rho^2}. \quad (\text{A6})$$

This is why we keep D_b as a leading-order effect but consider D_a to be subleading.

-
- [1] R. Aaij *et al.* (LHCb Collaboration), *Phys. Rev. Lett.* **122**, 222001 (2019).
- [2] H.-X. Chen, W. Chen, and S.-L. Zhu, *Phys. Rev. D* **100**, 051501 (2019).
- [3] R. Chen, Z.-F. Sun, X. Liu, and S.-L. Zhu, *Phys. Rev. D* **100**, 011502 (2019).
- [4] M.-Z. Liu, F.-Z. Peng, M. Sánchez Sánchez, and M. P. Valderrama, *Phys. Rev. D* **98**, 114030 (2018).
- [5] M.-Z. Liu, Y.-W. Pan, F.-Z. Peng, M. Sánchez Sánchez, L.-S. Geng, A. Hosaka, and M. Pavon Valderrama, *Phys. Rev. Lett.* **122**, 242001 (2019).
- [6] C. W. Xiao, J. Nieves, and E. Oset, *Phys. Rev. D* **100**, 014021 (2019).
- [7] M. Pavon Valderrama, *Phys. Rev. D* **100**, 094028 (2019).
- [8] T. Burns and E. Swanson, *Phys. Rev. D* **100**, 114033 (2019).
- [9] M.-L. Du, V. Baru, F.-K. Guo, C. Hanhart, U.-G. Meißner, J. A. Oller, and Q. Wang, *Phys. Rev. Lett.* **124**, 072001 (2020).
- [10] J.-J. Wu, R. Molina, E. Oset, and B. S. Zou, *Phys. Rev. Lett.* **105**, 232001 (2010).
- [11] J.-J. Wu, R. Molina, E. Oset, and B. S. Zou, *Phys. Rev. C* **84**, 015202 (2011).
- [12] J.-J. Wu and B. S. Zou, *Phys. Lett. B* **709**, 70 (2012).
- [13] C. W. Xiao, J. Nieves, and E. Oset, *Phys. Rev. D* **88**, 056012 (2013).
- [14] W. L. Wang, F. Huang, Z. Y. Zhang, and B. S. Zou, *Phys. Rev. C* **84**, 015203 (2011).
- [15] Z.-C. Yang, Z.-F. Sun, J. He, X. Liu, and S.-L. Zhu, *Chin. Phys. C* **36**, 6 (2012).
- [16] M. Karliner and J. L. Rosner, *Phys. Rev. Lett.* **115**, 122001 (2015).
- [17] M. I. Eides, V. Y. Petrov, and M. V. Polyakov, *Mod. Phys. Lett. A* **35**, 2050151 (2020).
- [18] Z.-G. Wang, *Int. J. Mod. Phys. A* **35**, 2050003 (2020).
- [19] G. Yang, J. Ping, and J. Segovia, *Phys. Rev. D* **101**, 074030 (2020).
- [20] J. Ferretti and E. Santopinto, *J. High Energy Phys.* **04** (2020) 119.
- [21] F. Stancu, *Phys. Rev. D* **101**, 094007 (2020).
- [22] L. Geng, J. Lu, and M. P. Valderrama, *Phys. Rev. D* **97**, 094036 (2018).
- [23] M. Bawin and S. Coon, *Phys. Rev. A* **67**, 042712 (2003).
- [24] E. Braaten and D. Phillips, *Phys. Rev. A* **70**, 052111 (2004).
- [25] H. W. Hammer and B. G. Swingle, *Ann. Phys. (Amsterdam)* **321**, 306 (2006).
- [26] V. Efimov, *Phys. Lett.* **33B**, 563 (1970).
- [27] R. Aaij *et al.*, *Phys. Rev. Lett.* **115**, 072001 (2015).
- [28] U. van Kolck, *Nucl. Phys. A* **645**, 273 (1999).
- [29] J.-W. Chen, G. Rupak, and M. J. Savage, *Nucl. Phys. A* **653**, 386 (1999).
- [30] M. Pavon Valderrama, *Eur. Phys. J. A* **56**, 109 (2020).
- [31] A. V. Manohar and M. B. Wise, *Nucl. Phys.* **B399**, 17 (1993).
- [32] A. F. Falk and M. E. Luke, *Phys. Lett. B* **292**, 119 (1992).
- [33] P. L. Cho, *Nucl. Phys.* **B396**, 183 (1993); **B421**, 683(E) (1994).
- [34] J.-X. Lu, L.-S. Geng, and M. P. Valderrama, *Phys. Rev. D* **99**, 074026 (2019).
- [35] P. L. Cho, *Phys. Rev. D* **50**, 3295 (1994).
- [36] S. Ahmed *et al.* (CLEO Collaboration), *Phys. Rev. Lett.* **87**, 251801 (2001).
- [37] A. Anastassov *et al.* (CLEO Collaboration), *Phys. Rev. D* **65**, 032003 (2002).
- [38] H.-Y. Cheng and C.-K. Chua, *Phys. Rev. D* **92**, 074014 (2015).
- [39] T. Aaltonen *et al.* (CDF Collaboration), *Phys. Rev. D* **84**, 012003 (2011).
- [40] M. Tanabashi *et al.* (Particle Data Group), *Phys. Rev. D* **98**, 030001 (2018).

- [41] U. van Kolck, *Eur. Phys. J. A* **56**, 97 (2020).
- [42] C. Bertulani, H. Hammer, and U. Van Kolck, *Nucl. Phys. A* **712**, 37 (2002).
- [43] M. C. Birse, J. A. McGovern, and K. G. Richardson, *Phys. Lett. B* **464**, 169 (1999).
- [44] F.-Z. Peng, M.-Z. Liu, M. Sánchez Sánchez, and M. P. Valderrama, *Phys. Rev. D* **102**, 114020 (2020).
- [45] R. Chen, A. Hosaka, and X. Liu, *Phys. Rev. D* **96**, 116012 (2017).
- [46] M.-Z. Liu, T.-W. Wu, M. Sánchez Sánchez, M. P. Valderrama, L.-S. Geng, and J.-J. Xie, [arXiv:1907.06093](https://arxiv.org/abs/1907.06093).
- [47] T. J. Burns, *Eur. Phys. J. A* **51**, 152 (2015).
- [48] Y. Shimizu, Y. Yamaguchi, and M. Harada, [arXiv:1904.00587](https://arxiv.org/abs/1904.00587).
- [49] Y. Yamaguchi, H. García-Tecocoatzi, A. Giachino, A. Hosaka, E. Santopinto, S. Takeuchi, and M. Takizawa, *Phys. Rev. D* **101**, 091502 (2020).
- [50] E. Epelbaum, U. G. Meissner, W. Gloeckle, and C. Elster, *Phys. Rev. C* **65**, 044001 (2002).